Geometry and evolution of rift-margin, normal-fault–bounded basins from gravity and geology, La Paz–Los Cabos region, Baja California Sur, Mexico

Melanie M. Busch[1], J Ramón Arrowsmith[1], Paul J. Umhoefer[2], Joshua A. Coyan[1], Sara J. Maloney[2], and Genaro Martínez Gutiérrez[3]
[1]SCHOOL OF EARTH AND SPACE EXPLORATION, ARIZONA STATE UNIVERSITY, P.O. BOX 871404, TEMPE, ARIZONA 85287, USA
[2]DEPARTMENT OF GEOLOGY, NORTHERN ARIZONA UNIVERSITY, CAMPUS BOX 4099, FLAGSTAFF, ARIZONA 86011, USA
[3]DEPARTAMENTO DE GEOLOGÍA MARINA, UNIVERSIDAD AUTÓNOMA DE BAJA CALIFORNIA SUR, LA PAZ, BCS 23080, MEXICO

ABSTRACT

The southern end of the Baja California peninsula is cut by a north-striking, left-stepping, active, normal-fault system—the marginal fault system of the oblique-divergent plate boundary within the Gulf of California. We conducted gravity surveys across the normal-fault–bounded basins, and, along with optically stimulated luminescence dating of offset piedmont surfaces and geologic data, we estimated fault-slip rates and assessed fault patterns across basins, gaining insight into basin evolution to better understand the role of upper-crustal processes during development of an obliquely rifted plate margin. Gravity surveys across the La Paz, San Juan de los Planes, and San José del Cabo basins revealed basin depths ranging from ~500 to 3000 m. The La Paz basin is a half graben with two smaller basins that reflect the two main east-dipping splays of the Carrizal fault. Within the San Juan de los Planes and San José del Cabo basins, there are buried faults, indicating that during the early stages of basin formation, strain was distributed across these smaller intrabasin faults prior to development of the basin-bounding faults. Slip rates coupled with basin depths suggest that the La Paz and San Juan de los Planes basins began forming ca. 2–5 Ma, overlapping in time with the formation of the main plate boundary at this latitude. The San José del Cabo basin has the greatest depth to bedrock (1.6–2.7 km), signifying that it accommodates a greater slip rate or a longer duration of slip than the other faults within this system.

LITHOSPHERE; v. 3; no. 2; p. 110–127; Data Repository item 2011054. doi: 10.1130/L113.1

INTRODUCTION

Continental rifts result from the breakup and extension of continental lithosphere. As the continental blocks separate, broad zones of continental deformation will eventually localize to become oceanic spreading centers, creating new oceanic crust. Some continental rifts are characterized by plate divergence that is oblique to the rift trend. In these oblique-divergent settings, often strain is accommodated by the partitioning of rift-perpendicular extension and rift-parallel shear (Withjack and Jamison, 1986). Many studies of oblique rifting use numerical models or experiments to predict the strain patterns that are likely to emerge with different angles of rift obliquity (e.g., Withjack and Jamison, 1986; Tuckwell et al., 1998; Clifton et al., 2000; Clifton and Schlische, 2001, 2003; McClay et al., 2002). In general, these studies indicate that a range of fault geometries can develop. Additionally, they predict the direction of motion accommodated by these faults, as well as the orientation of the faults with respect to the rift trend. For the Gulf of California oblique-divergent rift, in addition to the transform faults and short spreading centers in the main zone of deformation, these models predict the presence of normal faults that strike oblique to the main zone of deformation and form on the margin of the rift (Withjack and Jamison, 1986). The oblique-divergent rift within the southern Gulf of California manifests sustained oblique extension along the continental-oceanic transition with active normal faulting in a left-stepping array.

Previous studies of extended regions have provided insight into normal-fault behavior and rift basin formation, guiding the way in which we interpret our data. Extension is often accommodated by slip along relatively planar normal faults dipping 30°–60°. These faults are often arranged into fault arrays of similar slip sense and dip (e.g., Jackson and White, 1989). Normal faults in the same region generally dip in the same direction such that they do not cross, because crossing would cause the intersected faults to lock and become inactive (Jackson and McKenzie, 1983). These similarly dipping faults can slip and rotate in a domino-like fashion in cross section (e.g., Jackson and McKenzie, 1983; Jackson and White, 1989), eventually causing the fault to rotate out of a favorable angle for slip. Consequently, a new generation of steeper faults may form (Anderson, 1951). This progression of domino-style faulting, rotation, and new fault formation leads to formation of asymmetric half grabens in which footwall uplift and corresponding hanging-wall subsidence are greatest along the fault scarp and decrease away from the fault (e.g., Jackson and White, 1989). Additionally, the amount of uplift and subsidence along a fault varies along strike. Fault displacement, and therefore footwall uplift and hanging-wall subsidence, is greatest at the center of a segment and decreases toward the ends of a segment (e.g., Burbank and Anderson, 2001; Densmore et al., 2004). Extensional basins and their bounding normal faults may first begin as numerous small faults. Over time, as the extension increases, some of the faults link to become larger faults. Those faults in the shadow zones of the larger, linked structures become inactive. Strain becomes localized along the larger faults, which eventually become the border fault zones of graben and half-graben depocenters (Gupta et al., 1998).

In addition to the evolution of the fault array, the surrounding landscape and geomorphic and sedimentary systems develop and are partitioned by the structural arrangement of the fault system and the relative rates of slip along the faults. Geomorphic response to high slip rates along relatively isolated faults will establish a

landscape with clear associations between surface displacements and process (steep escarpment drainages, longer, lower-gradient drainages flowing off the back side of the hanging wall around the fault tip to the sedimentary basin, and corresponding depocenters reflecting high subsidence at the center of the fault; e.g., Gupta et al., 1998; Densmore et al., 2004). On the other hand, low-slip-rate, long-lived, normal-fault arrays may see more complex landscapes developed across them that are equally sensitive to regional gradients, such as continental to marine (elevation and process), as well as to the local, less coherent and lower-magnitude surface displacements due to fault slip along the interacting elements of the fault array (e.g., Gupta et al., 1998; Densmore et al., 2004).

An important control on the degree of distribution of the marginal system in a rift may be the gradients in topography, crustal thickness, and material properties along the edge of the rift system. Observations from Reykjanes peninsula of Iceland (e.g., Clifton and Schlische, 2003), the Gulf of Suez (e.g., Bosworth et al., 2005), and the Gulf of California (e.g., Lizarralde et al., 2007) motivate this hypothesis. It also has been explored with scaled laboratory experiments and numerical models (e.g., Tuckwell et al., 1998; Clifton and Schlische, 2003), which clearly demonstrated a partitioning of deformation rate and style from the high-rate, extensional normal faults and perpendicular transfer faults of the rift core to low-rate, distributed en echelon faults oblique to the rift in the transition zone.

The Gulf of California, a proto-oceanic trough (Ingersoll and Busby, 1995), is undergoing active transtensional continental rifting along an oblique-divergent plate boundary. Deformation in this region is accommodated by both strike-slip and normal-fault systems (e.g., Angelier et al., 1981; Fletcher and Munguía, 2000; Umhoefer et al., 2002; Plattner et al., 2007). The axis of the Gulf of California is marked by long, right-lateral strike-slip faults separated by shorter spreading centers and is referred to as the gulf-axis system. Adjacent to the gulf on the west, the east side of the southern tip of the Baja California peninsula hosts an onshore to offshore fault array of roughly north-striking, left-stepping, mostly east-dipping, normal faults known as the gulf-margin system (Fletcher and Munguía, 2000) (Fig. 1).

The onset of seafloor spreading in the southern Gulf of California at 6–2.4 Ma (Lizarralde et al., 2007; Umhoefer et al., 2008) was not accompanied by the cessation of continental rifting and the complete localization of the Pacific–North American plate boundary through the axis of the gulf (DeMets, 1995; Fletcher and Munguía, 2000; Plattner et al., 2007; Lizarralde et al., 2007). This region, therefore, provides the opportunity to study fault system development at a critical time during the rift-to-drift transition, when oceanic spreading has begun yet continental rifting is still active. The spreading rate across the Alarcón rise in the southern Gulf of California is slower than that of the Pacific–North American plate boundary (~90% of total), indicating that structures in addition to the transform faults and spreading centers in the gulf also accommodate deformation in this region (DeMets, 1995; Fletcher and Munguía, 2000; Plattner et al., 2007). Seismicity (e.g., Munguía et al., 2006) and geomorphic relationships (Fletcher and Munguía, 2000; Busch et al., 2006, 2007; Maloney et al., 2007) indicate that the array of normal faults rupturing the southern end of the Baja California peninsula are active and act as a weak distributed shear zone that contributes to translating the Baja California peninsula blocks away from mainland Mexico (Plattner et al., 2007). The gulf-margin is a zone of distributed extension as well as decreasing elevation and thinning crust (Lizarralde et al., 2007).

Whereas the gulf-margin fault array provides a relatively minor contribution to the overall plate divergence occurring in the region, these normal faults control the topography of the southern tip of the Baja California peninsula and produce moderate-sized earthquakes (Fletcher and Munguía, 2000). The faults bound prominent Quaternary basins and offset Quaternary alluvial deposits (Fletcher and Munguia, 2000; Busch et al., 2006, 2007; Maloney

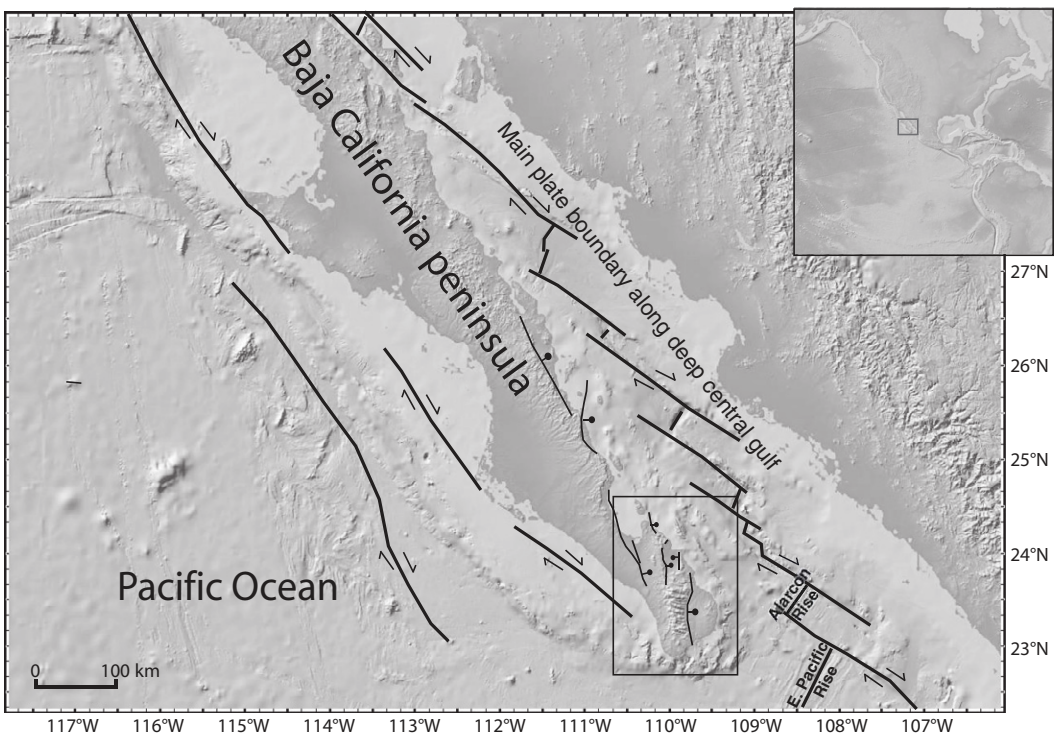

Figure 1. Map of the Gulf of California region showing the major fault systems that contribute to transtensional rifting. The gulf-axis system runs up the center of the Gulf of California. The gulf-margin system is situated along the southwest margin of the gulf. The borderland system is located offshore along the western side of the Baja California peninsula. Box on southern end of peninsula indicates focus of this study. Box on inset map indicates location of study area with respect to North and South America.

et al., 2007). By studying the onshore normal-fault array along the southwest margin of the Gulf of California, we are able to quantitatively assess the behavior of rift-margin normal faulting in a transitional stage of development of an obliquely rifted margin. More specifically, we can estimate the timing of the development of this system and the slip synchroneity among individual faults as well as gain insight into the evolution of the normal-fault–bounded basins. We can also make interpretations about the geometry of faults across the basins and the fault patterns in graben and half graben at the margin of an oblique rift.

In this paper, we present the results of reconnaissance-level gravity surveys across three major normal-fault–bounded basins in the La Paz–Los Cabos transect of the Baja California peninsula. The studied basins include the La Paz basin, bounded on the west by the Carrizal fault; the San Juan de los Planes basin, bounded on the west and east by the San Juan de los Planes fault and the La Gata fault, respectively; and the San José del Cabo basin, bounded on the west by the San José del Cabo fault (Fig. 2). All of these are active normal faults. The purpose of our gravity surveys was to determine the depth to bedrock and geometry of the individual basins. These gravity data along with our own and compiled geologic mapping allow us to speculate on the presence and location of major faults buried within the basins, as well as the relative total slip along these faults.

We also present optically stimulated luminescence (OSL) dates of Quaternary units along two of the major normal faults (San Juan de los Planes and El Carrizal; Fig. 2). We obtained dates from samples that were collected from the youngest Quaternary units that had been offset by faulting to constrain the timing of recent activity along the faults. Coupling this known timing of most recent activity with average scarp heights, as determined by detailed mapping, allows us to estimate late Quaternary slip rates along these faults. Integrating estimates of basin depths and geometries with slip rates enables us to characterize not only the histories of the individual basins, but also the behavior of this rift-marginal fault system as a whole. These data allow us to compare basin depths and slip rates such that we can make general interpretations about the synchroneity, or lack thereof, of basin formation and relative activity along the major normal faults, providing a broad view of system behavior.

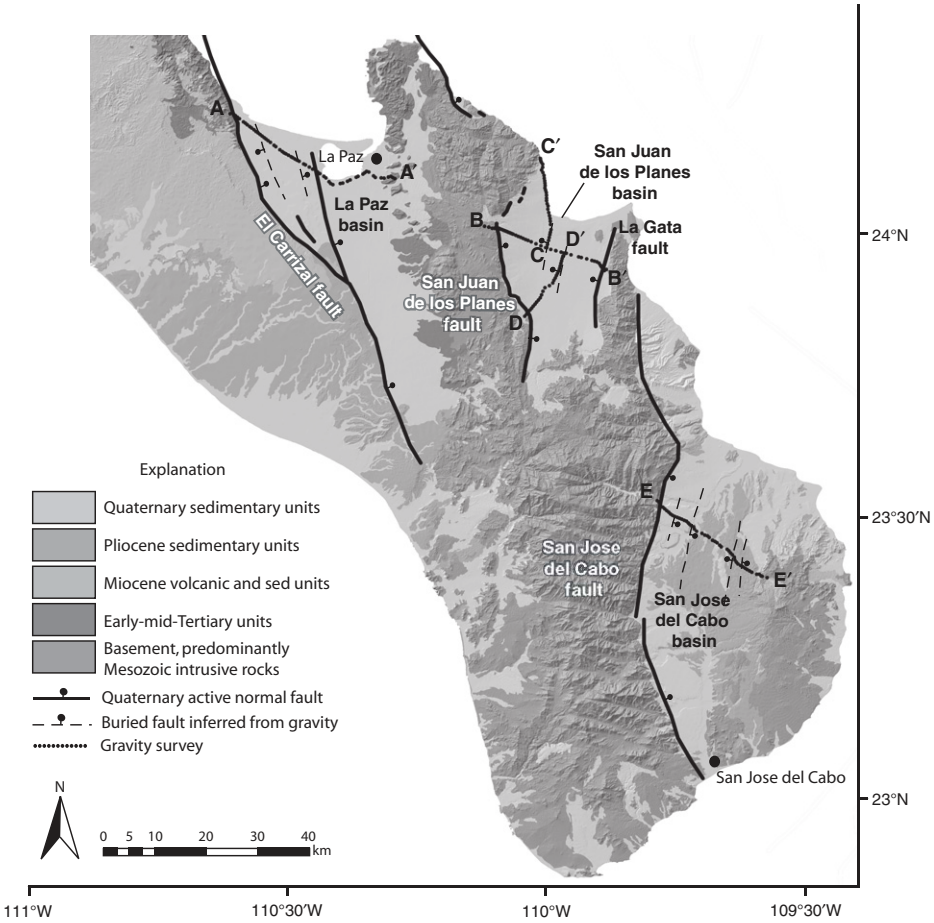

Figure 2. Geologic map of the southern end of the Baja California peninsula highlighting the location of major normal faults and their hanging-wall basins, as well as locations and orientations of gravity surveys across major normal-fault–bounded basins. Solid lines show Quaternary active normal faults. Dashed lines in basins show intrabasin fault locations inferred from gravity, with balls on downthrown block. Geology was modified from INEGI (1987). Fault traces are from INEGI (1987); Busch et al. (2006, 2007); and Maloney et al. (2007).

REGIONAL TECTONIC SETTING

Throughout most of the Cenozoic, the west coast of North America at the latitude of Baja California was the site of a subduction zone in which the Farallon plate was subducting eastward beneath western North America (Stock and Hodges, 1989). Circa 25 Ma, as the Farallon plate continued to be subducted and consumed, the Pacific plate, located west of the Farallon plate, came into contact with North America and began subducting beneath the North American plate, initiating the development of the Mendocino and Rivera triple junctions along southern California and northern Baja California (Atwater, 1970; Stock and Hodges, 1989). As subduction of the Pacific plate continued, the Mendocino triple junction moved northward, while the Rivera triple junction moved southward, lengthening the right-lateral transform plate boundary that had developed between the Pacific plate and North American plate (Stock and Hodges, 1989). This right-lateral system marked the early stages of the San Andreas fault system (Atwater, 1970).

Between ca. 20 and 12 Ma, a series of microplates formed along most of Baja California; the microplates were subsequently captured by the Pacific plate, and the former trench developed into a right-lateral strike-slip fault zone, the Tosco-Abreojos fault (Stock and Hodges, 1989; Stock and Lee, 1994). Between 12 and 6 Ma, NNW- and N-striking normal faults developed east of the Tosco-Abreojos fault, adjacent on the west to the region of the present-day Gulf of California (Stock and Hodges, 1989; Hausback, 1984; Umhoefer et al., 2002). The normal-fault–dominated gulf-margin system was either part of regional strain partitioning between the future Gulf of California region and the Tosco-Abreojos strike-slip fault to the west (Stock and Hodges, 1989), or the gulf-margin system has been part of a complex intragulf transtensional fault system since 12 Ma (Fletcher et al., 2003, 2007). The modern regime of oblique divergence began ca. 6 Ma as transform faults

separated by small rift basins began to form in the present-day Gulf of California, while activity began to diminish along the Tosco-Abreojos system (Fletcher and Munguía, 2000; Oskin et al., 2001). By 3.6–2.4 Ma, new oceanic crust was forming along the Alarcón Rise, the southernmost spreading center in the Gulf of California (DeMets, 1995; Umhoefer et al., 2008) (Fig. 1). The Gulf of California continues to be a region of oblique-divergent continental rifting (Fletcher and Munguia, 2000; Umhoefer et al., 2002; Mayer and Vincent, 1999; DeMets, 1995).

METHODS

Gravity Instrumentation and Data Acquisition

Three gravity lines were completed across the San Juan de los Planes basin: a central line trending roughly perpendicular to the axis of the basin, a northern line trending subparallel to the basin axis, and a southern line also trending subparallel to the basin axis. Both the La Paz basin and the San José del Cabo basin were each crossed by a single gravity line (Fig. 2). The geodetic location of each gravity observation station was measured to centimeter-scale accuracy with real-time kinematic Global Positioning System (GPS). The relative gravity at each observation station was measured with a LaCoste and Romberg Model G gravity meter to an accuracy of 0.01 mGal. This instrument has a long-term drift of less than 0.5 mGal/mo (LaCoste and Romberg, 2004).

The lengths of the gravity lines range from approximately 15 km for the northern line across the San Juan de los Planes basin to over 37 km for the line across the La Paz basin. The gravity observation stations were spaced ~500 m apart, but some were as close as 200 m apart and as far as 1000 m apart along the central San Juan de los Planes line. The extremes of all lines were anchored on crystalline bedrock, with the exception of the southern end of the northern Los Planes line and the northern end of the southern Los Planes line, which were anchored on the central Los Planes line (Fig. 2).

A local base station was designated for each gravity line. The relative gravity at the local base stations was measured at least every 2 h during the surveys to account for drift. In addition to the local base stations, each gravity line was tied to a regional base station with a known gravity value, enabling the relative gravity measurements to be converted to absolute measurements. Not only was the relative gravity measured at stations along the predetermined line, but it was also measured at bedrock outcrops surrounding the survey lines, providing additional data from which to calculate the regional trend of the gravitational anomaly.

Gravity Data Processing and Modeling

The raw values measured by the gravimeter were corrected through a number of steps to obtain residual values. These residual values were then modeled to interpret general basin depth and geometry, including subsurface structures. Initial data processing included converting the dial reading to values in mGal and correcting for drift. Further corrections included a latitude correction, free-air correction, Bouguer correction, and terrain correction, which were all taken into account in calculating the complete Bouguer anomaly (CBA). Finally, a regional anomaly was determined and was subtracted from the CBA to obtain the residual gravity anomaly. Of these corrections, calculation of the terrain correction and regional anomaly merit further discussion. As a general reference in this data reduction, we followed Burger et al. (2006) and Sharma (1997).

The terrain corrections were computed using the program RasterTC from Geophysical Software. User-provided gravity station locations and a grid of terrain elevations were used to correct for the effect of the terrain surrounding gravity measurements from a user-specified radius of R_{min} to R_{max} (Cogbill, 1990). The area between R_{min} and R_{max} was divided into an inner zone and an outer zone, which is separated by radius R_{med}. Corrections within the area between R_{min} and R_{med} were computed by numerically integrating a smooth surface that fit the digital elevation data. Between R_{med} and R_{max}, the digital elevation data were integrated using the rectangular rule (Cogbill, 1990). For the present study, we set R_{min}, R_{med}, and R_{max} to 10 m, 500 m, and 20,000 m, respectively. Our gridded terrain data came from a 30 m digital elevation model (DEM) that was interpolated from topographic contour maps produced with stereo photogrammetry by Instituto Nacional de Estadística y Geografía (INEGI). The DEMs compare well with Shuttle Radar Topography Mission 90 m data. The integral effect of the terrain correction results from mean values, therefore negating errors in elevations, assuming there is no bias in the elevation data.

Because our interest was the shape of the sedimentary basins, we needed to remove the effect of longer-wavelength (deeper) density variations by determining a "regional" gravity pattern from which the CBA would be subtracted at each station to compute the "residual" gravity measurement, which we then used in our interpretation. To compute the regional anomaly, linear interpolation was used to compute a surface through gravity values obtained from bedrock stations within the region of the gravity line. The interpolated regional value was then determined for each of the gravity stations.

Gravity data (see GSA Data Repository[1]) were modeled in two dimensions (2-D) with GM-SYS gravity and magnetic modeling software from Northwest Geophysical Associates, Inc., using a forward modeling approach. Residual gravity values were entered into GM-SYS, and an initial basin model was created based on known geology in the region (INEGI, 1987; Busch et al., 2006, 2007; Maloney et al., 2007). The unit thicknesses and basin geometry were then modified until minimal error was achieved between the model anomaly and the observed anomaly. Because gravity data tend to produce nonunique interpretations, each gravity line was modeled in various ways, varying basin geometry and basin-fill density, while maintaining similarly low errors for each model. The models created for each basin progressed from having a smooth bedrock–basin-fill interface to a highly irregular bedrock–basin-fill interface. We favor the intermediate models as the most likely candidates for the actual subsurface geometries (Fig. 3). The models take into account data collected from our own mapping efforts and structural measurements along the San Juan de los Planes and Carrizal fault zones (Busch et al., 2006, 2007; Maloney et al., 2007).

Simple two-layer models were constructed for the San Juan de los Planes basin and the San José del Cabo basin, where granite bedrock is overlain by basin-fill sediments. The La Paz basin was modeled several ways, progressing from a simple two-layer model, where granite bedrock is overlain by basin-fill sediments, to a four-layer model that has an added basal layer of gabbro, which intrudes the granite, as well as a layer of volcaniclastic rocks situated between the basin-fill sediments and the granite. This four-layer model was based on the work of Gallardo et al. (2005) as well as regional geologic mapping from INEGI (1987) and Hausback (1984). We chose to present representative models that are simple and most plausible based on the regional geology, because our goal is to understand the net basin geometry and the most prominent features within the basin. Our conceptions of normal-fault behavior and mechanics guided our interpretations of normal-fault dip angle, dip direction, and spacing as we

[1]GSA Data Repository Item 2011054, table of gravity and GPS survey data, is available at www.geosociety.org/pubs/ft2011.htm, or on request from editing@geosociety.org, Documents Secretary, GSA, P.O. Box 9140, Boulder, CO 80301-9140, USA.

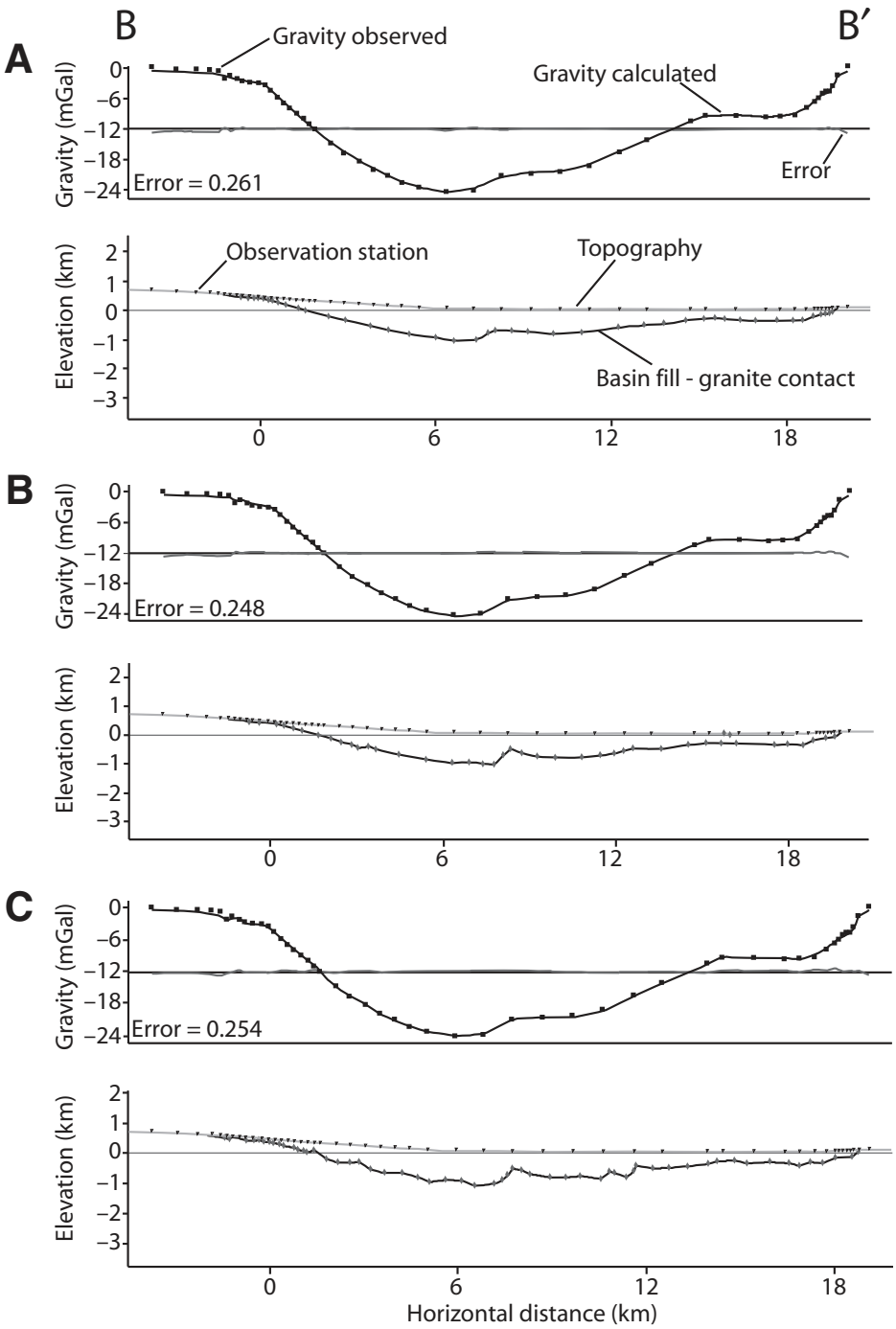

Figure 3. Three models of the gravity data across the San Juan de los Planes basin (B–B′). For each scenario, the top panel shows gravity observations and model fit, and the bottom panel shows the structural model. (A) Smooth granite–basin-fill interface geometry; (B) intermediate granite–basin-fill interface geometry; and (C) irregular granite–basin-fill interface geometry. Difference in misfit between observed and modeled residual gravity values among the three models is negligible. See Figure 2 for location.

transformed our models into geologic cross sections (see following for results and discussion of models).

Unit densities were designated based on the gravity and magnetic studies of Gallardo et al. (2005), which took place on the southern end of the Baja California peninsula, as well as previous gravity work completed by Tatlow (2000) near Phoenix, Arizona, which investigated rocks similar in type and age to those found in the La Paz–Los Cabos transect of the Baja California peninsula. For all basin models, the granite density is 2.67 g/cm^3, and the basin-fill density varies from 2.0 g/cm^3 to 2.2 g/cm^3. For the La Paz basin models, the gabbro density is 2.90 g/cm^3, and the Tertiary volcanic layer has a density of 2.47 g/cm^3. Basin-fill density is probably the major uncertainty. The 2.0–2.2 g/cm^3 range induces a typical variation in basin thickness of 500–1000 m.

Quaternary Geochronology and Fault-Slip Rates

In the course of our detailed mapping of the Quaternary sedimentary units, landforms, and fault traces along the San Juan de los Planes (Busch et al., 2007) and Carrizal fault zones (Maloney et al., 2007), we collected samples to be dated with OSL dating techniques (Table 1). The OSL dating method provides an estimate of the time when quartz or feldspar grains were last exposed to sunlight. It is thus a valuable tool for estimating the formation age of a Quaternary landform (e.g., Forman et al., 2000; Lian and Roberts, 2006). Prior to collecting our samples, we either dug pits from which to collect the sample, or we excavated back the wall of a natural drainage incision to expose a fresh face. We collected silt- and sand-sized sediment that had been buried at least 50 cm away from the closest exposed surface. Samples were collected in opaque cylinders that were quickly sealed until they were analyzed at the Utah State University Optically Stimulated Luminescence Laboratory.

Detailed geologic and geomorphic mapping along the San Juan de los Planes (Busch et al., 2007) and Carrizal (Maloney et al., 2007) fault zones guided selection of sample collection sites. We collected samples from Quaternary geomorphic surfaces adjacent to the fault zones. Along the San Juan de los Planes fault, samples from the youngest faulted Quaternary surface, as well as the oldest unit unaffected by faulting, were dated (Busch et al., 2008). These samples were strategically selected to bracket the time period of the most recent activity along the San Juan de los Planes fault. Scarp profiles were constructed across faulted geomorphic surfaces from which deposits were sampled in order to document scarp height and slope (Busch et al., 2007). We assume that the average scarp height represents the vertical offset magnitude, which we convert to vertical offset rate by dividing by the underlying deposit age. Because the faults have a steep dip, this vertical offset rate is likely similar to the dip-slip rate. Age estimates from both the youngest faulted surface as well was the oldest unfaulted

TABLE 1. OPTICALLY STIMULATED LUMINESCENCE (OSL) AGE INFORMATION

Sample no.	Field ID	Map unit	Sample location	Depth (m)	Grain size (μm)	H_2O (%)	Dose rate (Grays/ka)	Equivalent dose (Grays)	OSL age (ka)	Adjusted age* (ka)
USU-199	32207-2A	Qya_2	110.0655°W, 23.9870°N	1.05	63–250	0.2	2.05 ± 0.08	9.56 ± 5.25	4.65 ± 2.57	2.5 ± 2.5
USU-201	32107-1A	Qya_3	110.0684°W, 23.9851°N	0.50	75–250	0.1	3.09 ± 0.13	9.73 ± 4.80	3.15 ± 1.56†	4.0 ± 3.0
USU-170	41007-1A	Qya_4	110.0723°W, 23.9811°N	1.65	90–250	1.0	1.97 ± 0.08	26.36 ± 14.71	13.38 ± 1.75	16.2 ± 1.8
USU-169	41007-2A	Qya_4	110.0649°W, 23.9890°N	7.94	90–250	1.1	2.79 ± 0.12	39.38 ± 18.12	14.11 ± 6.53†	16.2 ± 1.8
USU-203	32207-3A	Qya_4	110.0842°W, 24.0249°N	0.50	75–250	0.5	2.16 ± 0.09	36.75 ± 5.29	16.99 ± 0.95	16.2 ± 1.8

Note: All samples are from the San Juan de los Planes fault zone.
*Adjusted with computer program OxCal v. 3.10 (Bronk Ramsey, 2001) and IntCal 2004 atmospheric data set (Reimer et al., 2004).
†Sample analyzed using a 3 s, 1% diode short shine to remove ultrafast signal (following Goble and Rittenour, 2006).

surface allow us to estimate a late Quaternary vertical offset rate range along the San Juan de los Planes fault (Busch et al., 2008).

Along the Carrizal fault zone, paleoseismic trenches were excavated, and faulted stratigraphy was documented (Maloney et al., 2007). OSL samples were collected from Quaternary units that bound the faulted layers. Additionally, total vertical separation of the faulted units was measured. The OSL dates date recent activity along the fault that, when coupled with the vertical separation of the units, was used to estimate a late Quaternary vertical offset rate range along the Carrizal fault (Maloney, 2009).

RESULTS

San Juan de los Planes Basin

Three lines were surveyed across the San Juan de los Planes basin revealing a maximum gravity anomaly of ~25 mGal and a maximum depth to bedrock of ~1.0–1.5 km (Fig. 4). The central line, trending subperpendicular to the long axis of the basin, was modeled in various ways, and despite the variations among the models, they all exhibit a similar asymmetry in which the deepest part of the basin is slightly west of center (Fig. 4, B–B′). A second prevalent feature present in all models is an intrabasin bedrock high, with ~0.5–1.0 km of relief, flanking the east side of the deepest part of the basin; it is interpreted to result from a relict, west-dipping normal fault. Certainly, other geological complexities will influence the gravity signal; however, they will they have the sharp surface signal that we have used to highlight possible faults only if they are as shallow as the inferred alluvium/bedrock interface we have modeled, or are unreasonably extreme in density contrast. The data from this central gravity line coupled with geologic mapping indicate that this basin is a graben, bounded by the San Juan de los Planes fault on the west and the La Gata fault on the east.

The N-S–trending line in the northern part of the basin did not reveal any significant bedrock structures along its length (Fig. 4, C-C′). The bedrock below this line shallows to the north, presumably because the line is intersecting the northern end of the fault zone obliquely, where activity has diminished, and, therefore, displacement is low. The N-S–trending line in the southern part of the basin revealed that the depth to bedrock decreases from the center of the basin toward the south (Fig. 4, D–D′). At the southern end of this gravity line, the basin shallows abruptly, providing subsurface evidence for the presence of a northeast-dipping normal fault. A corresponding 3–6-m-high scarp is observable on the surface. Based on gravity data, this fault has accommodated ~500 m of total slip.

La Paz Basin

The hanging wall of the Carrizal fault is the La Paz basin. The maximum gravity anomaly across the basin is ~10 mGal. The La Paz basin is the shallowest of the studied basins, with a maximum depth to bedrock of ~200–500 m, depending upon whether the two-layer or the four-layer gravity model is considered (Fig. 5). The two-layer model most simplifies the geology by grouping all rock units below the basin fill as a single bedrock unit. The three-layer model distinguishes the Tertiary volcanic unit from the granitic bedrock. The four-layer model includes a gabbroic intrusion, consistent with a regional gravity study completed by Gallardo et al. (2005). Additionally, grabbroic outcrops are present near the La Paz basin (INEGI, 1987; Gallardo et al., 2005). Because the subsurface geometry of the gabbro unit is unknown, it has been simplified in the four-layer model as a pillar-shaped unit intruding into the granite. Addition of the gabbroic unit to the gravity model improves the fit between the model and the observed gravity data on the eastern end of the gravity survey. All models predict the same general geometry and structure for the La Paz basin: a half-graben with two smaller basins separated by a bedrock high. The westernmost of the two smaller basins is controlled by the east-dipping Carrizal fault on its western side, whereas the easternmost basin is controlled by the east-dipping Centenario fault on its western side. All models depict the easternmost basin as the deeper of the two basins, with approximate maximum depths of 280 m, 350 m, and 490 m for the two-layer, three-layer, and four-layer models, respectively.

San José del Cabo Basin

One gravity line was surveyed across the San José del Cabo basin, revealing a maximum gravity anomaly of ~40 mGal and a maximum depth to bedrock ranging from 1.6 to 2.7 km as the basin-fill density is changed from 2.0 g/cm^3 to 2.2 g/cm^3, respectively. The gravity line stopped to the east at the first basin margin with Miocene strata unconformably set against Cretaceous granite (Martínez-Gutiérrez and Sethi, 1997; McTeague, 2006), and it did not continue across a 2-km-wide granite footwall to an east-dipping normal fault, nor the 3–4-km-wide Miocene half graben to the east (McTeague, 2006). The bedrock within the basin exhibits irregular topography (Fig. 6). Two bedrock features are robust in all models: an ~1-km-high, step-like feature on the western end of the basin, and an ~1–2-km-wide block of bedrock that rises ~1 km above the surrounding bedrock, located on the eastern side of the basin. Because these features are present in all models, and because they have significant relief, they are interpreted as fault blocks rather than paleotopography. The down-to-the-east normal fault that makes the small half graben east of our gravity line has copious evidence for Miocene activity (McTeague, 2006) and confirms that it is reasonable to infer Miocene normal faults buried in the basin.

Overall, both the gravity data and the regional geology lead us to the interpretation that this is a modified half graben. Along the western side of the basin, the high elevation of the footwall and sharply defined transition from the hanging wall to the footwall (San José del Cabo fault) compared to the more subdued bedrock topography on the eastern side of the basin and lack of fault scarp are indicative of a half-graben structure as the final basin structure we see today. However,

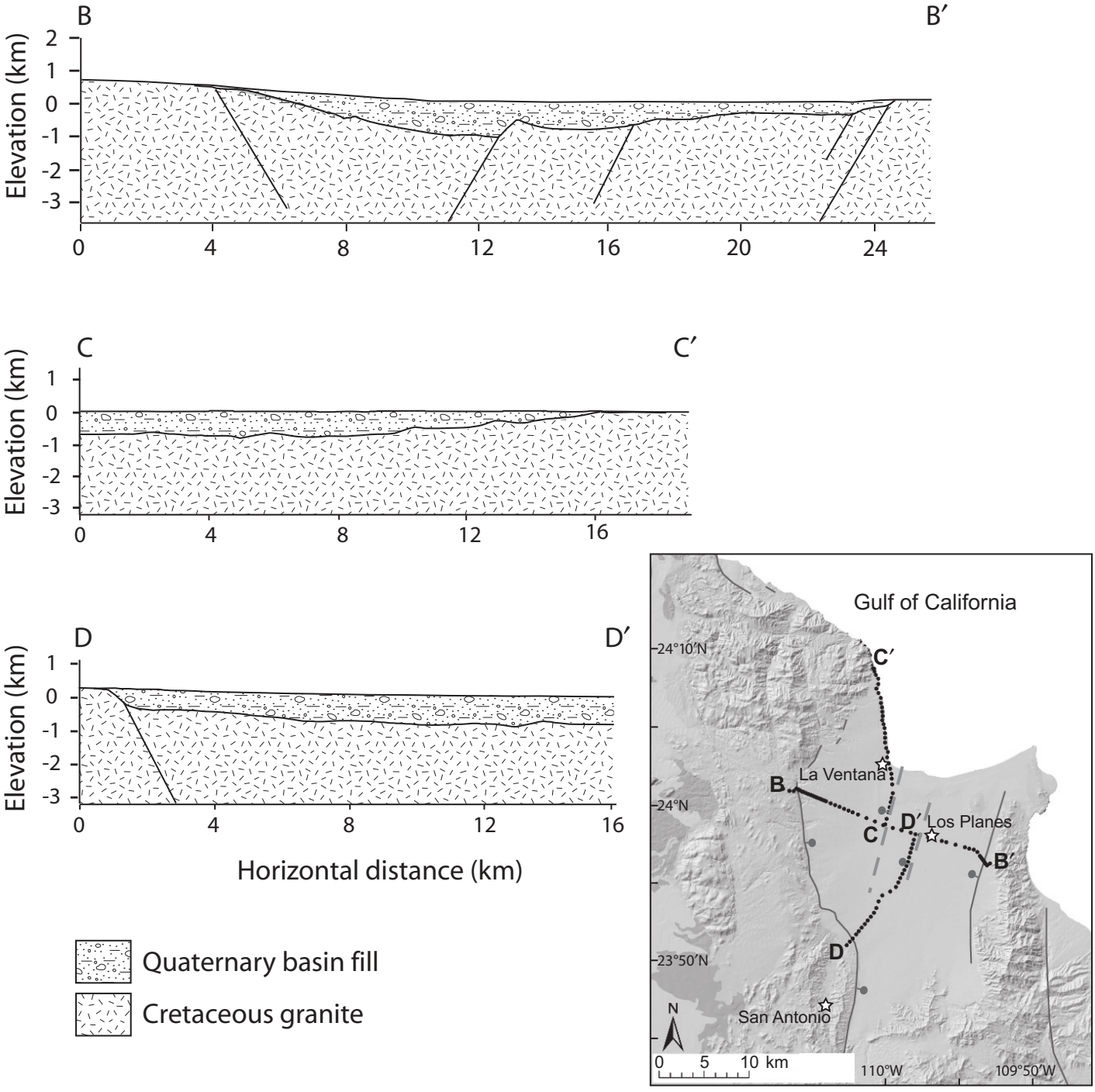

Figure 4. Simple geologic cross sections across the San Juan de los Planes basin, derived from gravity data and surface geology. Line B–B′ shows a basin that is a graben bounded by the San Juan de los Planes fault on the west and the La Gata fault on the east. Note the asymmetry where the deepest part of the basin is west of center and is flanked by an intrabasin bedrock high, with ~0.5–1.0 km of relief. Line C–C′ shows that bedrock in this section shallows to the north, presumably because the line is intersecting the northern end of the fault zone obliquely, where activity has diminished, and, therefore, displacement is low. Line D–D′ shows that the depth to bedrock decreases from the center of the basin toward the south. At the southern end of this gravity line, the basin shallows abruptly, providing subsurface evidence for the presence of a northeast-dipping normal fault that has accommodated ~500 m of total slip. Inset map shows gravity line locations (dotted lines). Solid lines show Quaternary active normal faults. Dashed lines in basin show intrabasin fault locations inferred from gravity, with balls on downthrown block.

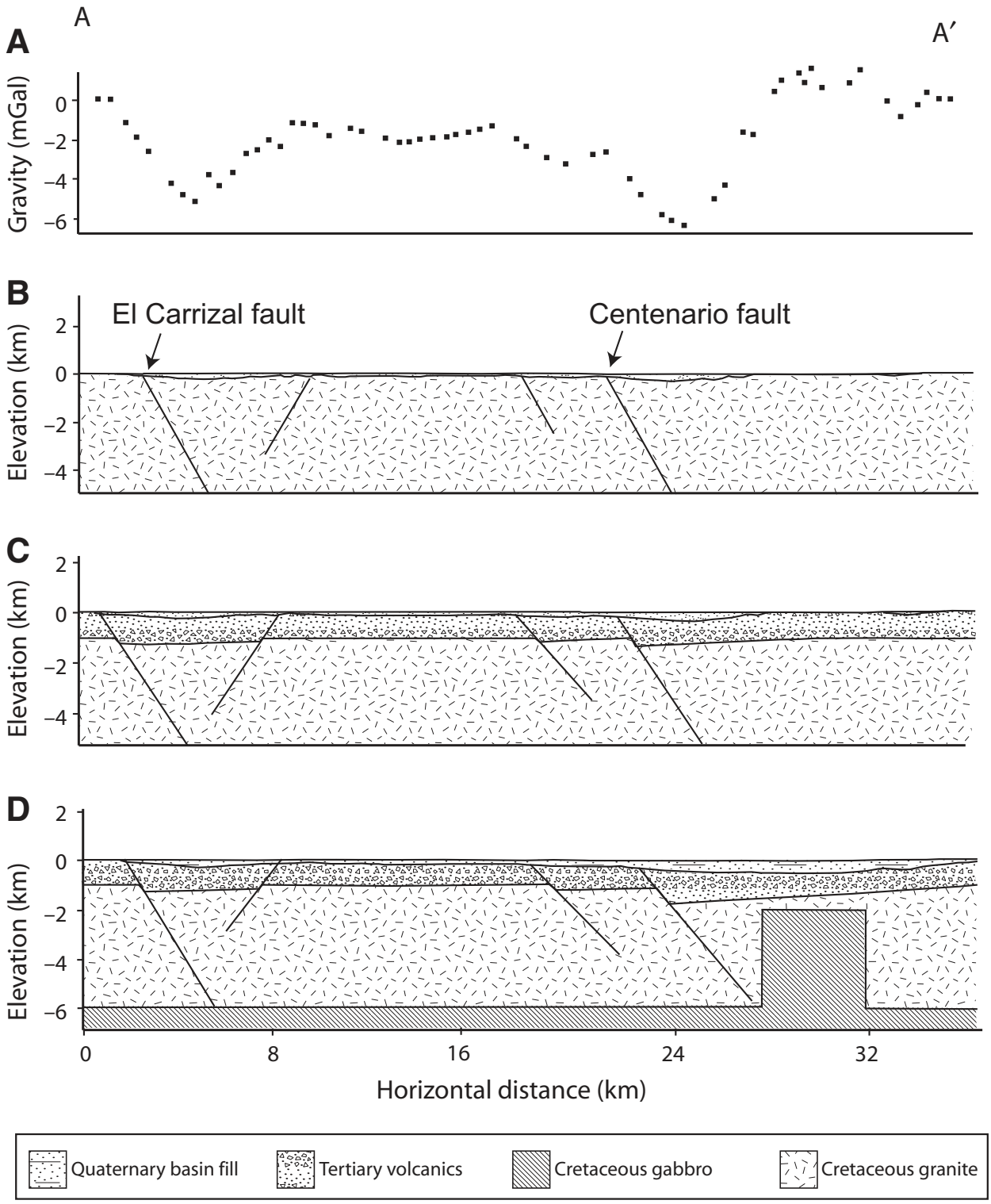

Figure 5. Simple geologic cross sections across the La Paz basin derived from gravity data and surface geology. See Figure 2 for gravity line location. (A) gravity observations; (B) two-layer model; (C) three-layer model; and (D) four-layer model, which best fits the observed gravity data. Addition of the gabbroic unit in the four-layer model is consistent with geology in the region (INEGI, 1987) as well as a regional gravity study by Gallardo et al. (2005). Pillar-like shape of gabbroic unit is for simplification because subsurface geometry unknown. The La Paz basin is the shallowest of the studied basins, with a maximum depth to bedrock of ~200–500 m. All models predict the same general geometry and structure for the La Paz basin: a half graben with two smaller basins separated by a bedrock high. The westernmost of the two smaller basins is controlled by the east-dipping Carrizal fault on its western side, whereas the eastern basin is controlled by the east-dipping Centenario fault on its western side. All models depict the easternmost basin as the deeper of the two basins.

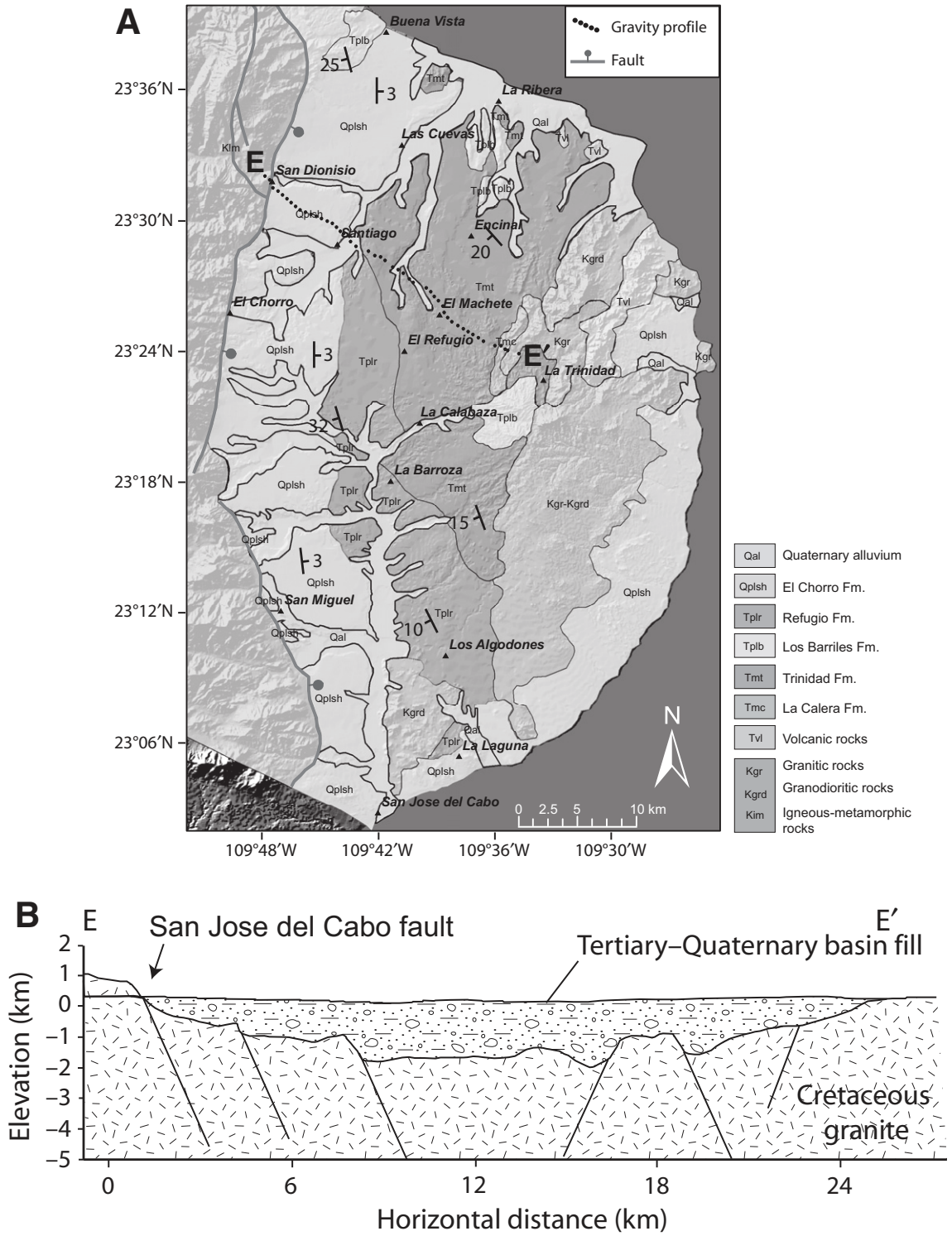

Figure 6. (A) Geologic map of the San José del Cabo basin from Martínez-Gutiérrez and Sethi (1997). (B) Cross section across the San José del Cabo basin derived from gravity data and surface geology. This half-graben basin contains a series of predominantly east-dipping, relict normal faults within the basin and is controlled by the east-dipping San Jose del Cabo fault on the west. Dashed footwall topography is representative of the high footwall elevation adjacent to the San Jose del Cabo fault (which in the range continues to 3 km elevation). The bedrock within the basin exhibits irregular topography, most notably an ~1-km-high, step-like feature on the western end of the basin and an ~1–2-km-wide block of bedrock that rises ~1 km above the surrounding bedrock, located on the eastern side of the basin.

according to our gravity model, the main older, down-to-the-east normal fault is ~6–7 km east of the present San José del Cabo fault, and that the initial half-graben boundary is buried near Santiago, which is also the western limit of the exposed Miocene marine stratigraphy. This half graben is modified by the eastern horst and the Miocene normal faults farther east of our gravity line (McTeague, 2006). The proposed buried eastern horst is mimicked by the prominent isolated granite high in the south-central basin north of San José del Cabo (Fig. 6). It is possible that the present western limit of marine strata in the basin is reflecting the early east-dipping normal fault buried near Santiago, which may control the boundary between terrestrial strata to the west and marine strata in the deeper half graben to the east. The older basin fill dips mainly to the west across the basin, confirming a general half-graben geometry that is fundamentally a Miocene to Pliocene feature. The Quaternary unit along the western basin dips only a few degrees east, and thickens to the west, both reflecting the stepping of faulting from Santiago to the present San José del Cabo fault perhaps in the Pliocene. The gentle east dips in the Quaternary alluvial fan (El Chorro Formation; Martínez-Gutiérrez and Sethi, 1997) may be original dips on an east-facing bajada that has since been incised by modern arroyos.

Fault-Slip Rates

OSL dates were adjusted with the radiocarbon calibration program OxCal (version 3.10) (Bronk Ramsey, 1995, 2001) such that the ages (weighted Gaussian-shaped probability distributions) associated with the oldest Quaternary geomorphic surface were combined, whereas the ages of the younger surfaces were adjusted using stratigraphic constraints (Bronk Ramsey, 2008). Based on these OSL dates (Table 1), the youngest faulted unit along the San Juan de los Planes fault is 16.2 ± 1.8 ka, and the oldest unfaulted unit is 4.0 ± 3.0 ka. These ages bracket the timing of fault slip. An average scarp height of ~4 m was determined from a series of scarp profiles constructed along the length of the fault zone (Busch et al., 2007). Maximum and minimum vertical offset rates along this fault are thus 1 mm/yr and 0.25 mm/yr, respectively (Busch et al., 2008). Paleoseismic trenching along the southern Carrizal fault revealed a total vertical separation of 2.2 m and an age bracket of most recent activity between 20.6 ka and 1.4 ka, leading to estimates of maximum and minimum offset rates of 1.6 and 0.11 mm/yr, respectively (Maloney, 2009).

We based our slip-rate calculations on the assumption of dip-slip motion only and did not take into account the possibility of oblique slip as various data suggest these are mainly N-S–trending normal faults. For example, focal mechanisms for earthquakes recorded from 1969 through 1995 across the La Paz transect show pure normal faulting along NW-striking faults and suggest strain partitioning across the gulf at this latitude (Fletcher and Munguía, 2000). Strain partitioning results from normal displacement along approximately N-S–striking faults on the southern end of the Baja California peninsula, strike-slip displacement along WNW-striking faults off the west coast of the peninsula, and oceanic spreading centers and transform faults within the Gulf of California. Additionally, faults observed in paleoseismic trenches across the Carrizal fault show fabrics consistent with normal offset (Maloney, 2009). Uplifted marine terraces on the footwall of the Carrizal fault suggest at least a major component of dip-slip motion (Buchanan, 2010; DeDiego-Forbis et al., 2004). Secondary faults in the footwall of the Carrizal fault exhibit dominantly dip-parallel sense of slip indicators (Drake, 2005). Additionally, the mapped geometry of the San Juan de los Planes and Carrizal faults exhibits the characteristic concave plan-view shape of known normal faults (Busch et al., 2007; Maloney et al., 2007).

DISCUSSION OF INFERRED BASIN GEOMETRIES

San Juan de los Planes Basin

Although the gravity models provide an estimate of a minimum total displacement along the basin-bounding faults, the modeled maximum depth to bedrock is probably a fair estimate of the total displacement along the San Juan de los Planes fault. Apatite and zircon fission-track analyses of samples from the footwall of the Los Planes fault ~6–8 km west of the fault zone yielded zircon and apatite fission-track ages ranging from 62 to 63 Ma and 48 to 53 Ma, respectively, and mean apatite track lengths of 12.74–13.02 µm (Fletcher et al., 2000). These data, indicating that this area experienced slow cooling throughout most of the Tertiary, coupled with the low footwall relief, ranging from ~600 to 1000 m, suggest that little exhumation and erosion of the footwall occurred during the Tertiary.

In the San Juan de los Planes basin, the maximum depth to bedrock is just northwest of center, asymmetric toward the San Juan de los Planes fault (Fig. 4, B–B′), possibly marking the location of basin inception, indicating that as the basin evolved, faulting moved outward to the presently active San Juan de los Planes and La Gata faults (Fig. 2). The location of maximum basin depth along the central gravity line occurs adjacent to a bedrock high that has been interpreted as bounded by a west-dipping fault. A second, more eastern, west-dipping fault has also been interpreted within the basin based on the geometry of the granite–basin-fill contact as well as surficial evidence discussed later herein. Fletcher and Munguía (2000) also acknowledged the existence of a fault within the center of the San Juan de los Planes basin, though they interpret it to be an active, east-dipping splay of the San Juan de los Planes fault, presumably to maintain continuity between this splay and the east-dipping Espíritu Santo fault farther north, to which they infer linkage. Whether one or both of the intrabasin faults is active is uncertain. A handful of recent seismic events (Munguía et al., 2006) within the basin provide modest evidence of active faulting. An ~150-m-wide, ~15-m-high crystalline bedrock knob protrudes from the basin sediments (Fig. 7); however, exposure of this knob may be purely erosional, resulting from the extensive axial drainage that flows northward, rather than from recent faulting.

The gravity survey in the southern part of the San Juan de los Planes basin suggested a fault at its southern end (Fig. 4, D–D′). This fault corresponds to an ~2-km-wide left step in the San Juan de los Planes fault (Busch et al., 2007). The total slip in this section of the fault is ~500 m. Gravity modeling suggests that this fault segment has the steepest gravity gradient of the faults surveyed, which might suggest that this segment formed more recently and/or slips at a higher rate than the other fault segments. Previous work on fault segmentation and linkage suggests that as individual smaller faults extend toward each other, they eventually link up to form a longer, continuous structure (e.g., Burbank and Anderson, 2001; Gawthorpe and Leeder, 2000). Given these gravity results, the San Juan de los Planes fault zone appears to exhibit this classic normal-fault behavior in which two fault segments linked up along strike and this step, or linkage, is the most recently active segment.

A thicker package of Quaternary sediment exists on the immediate hanging wall of the La Gata fault than that of the Los Planes fault (Fig. 4, B–B′). Additionally, the maximum depth to bedrock is located adjacent to the west-dipping intrabasin fault. These features imply higher activity (and thus greater subsidence, providing accommodation space for deposition) along the west-dipping faults than along the San Juan de los Planes fault. The gravity models suggest that the San Juan de los Planes fault may have formed more recently than the La Gata fault or that it slips at a lower rate. This inference is also consistent with

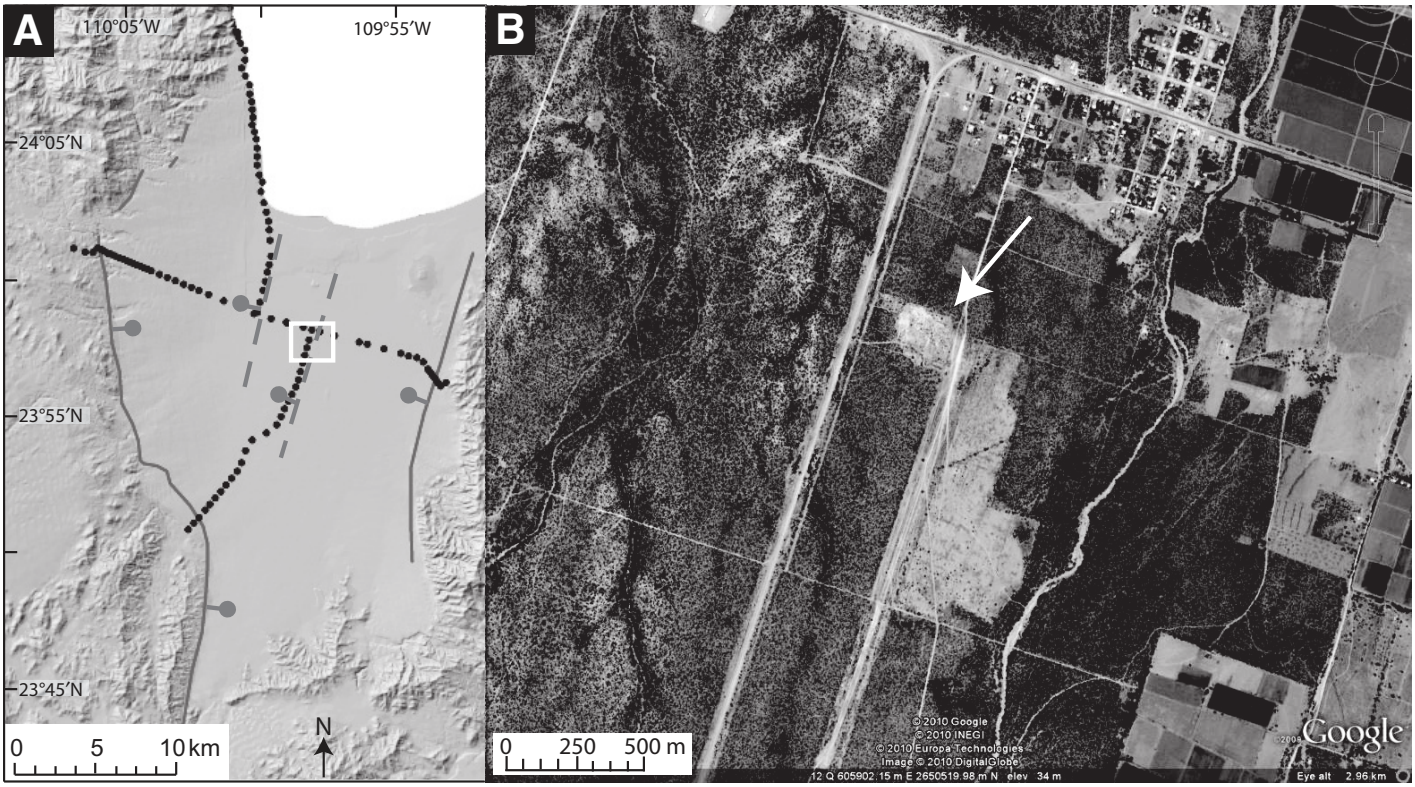

Figure 7. (A) Geologic map of San Juan de los Planes basin. White box on map indicates approximate location of aerial photograph. Solid lines show Quaternary active normal faults. Dashed lines in basin show intrabasin fault locations inferred from gravity, with balls on downthrown block. (B) Aerial photograph showing bedrock knob (indicated by arrow) protruding through basin sediments in the San Juan de los Planes basin. Geology is from INEGI (1987); fault traces are from Busch et al. (2007); satellite image is from Google Earth.

reconnaissance shallow-marine CHIRP (Compressed High Intensity Radar Pulse) observations, which showed 10–40 m scarps along the offshore continuation of the La Gata system (Arrowsmith et al., 2009).

Although more detailed mapping of the La Gata fault zone remains to be completed, it appears that the gravity line crosses the La Gata fault at a segment boundary, or salient, and so the total slip could be less along this section of the fault than along strike to the north or south, causing the eastern side of the basin to appear shallower than it actually is in other parts of the basin margin (Fig. 8). It is also possible that the gravity line crosses the La Gata fault at its southern end, assuming the La Gata fault continues to be active offshore to the north. In this case, the gravity survey would also show a relatively shallower portion of the basin. Resolution of these uncertainties requires more detailed mapping along the La Gata fault zone, more gravity observations, and obtaining offshore bathymetric and seismic-reflection or CHIRP data north of the San Juan de los Planes basin.

In general, the gravity models of the San Juan de los Planes basin are consistent with field observations (Busch et al., 2007). Drainage incision on the hanging wall of the San Juan de los Planes fault adjacent to the fault zone reveals thin Quaternary cover over the granite bedrock, ranging in thickness from a few meters to ~100 m (Fig. 9). Basin models based on the gravity data also show that the Quaternary sediment cover is thin (~10–200 m thick) within ~3 km into the hanging wall. The footwall topographic relief along the La Gata fault zone is higher than that along the Los Planes fault, and the transition from the hanging wall to the footwall is more sharply defined, indicating that the La Gata fault may be more active than the San Juan de los Planes fault. Gravity data are consistent with this observation, revealing a more well-defined fault in the subsurface bounding the eastern side of the basin than the west, as well as a thicker sediment package, as discussed previously. Another consistency between the observed geology and the gravity data is the prominent step in the southern end of the Los Planes fault zone, which can be observed on the surface and is resolved by the gravity data. These consistencies between the observed geology and the gravity data instill confidence in our gravity collection and analysis here and for the remaining two basins.

La Paz Basin

The onshore La Paz basin is unexpectedly shallow given the length of the bounding faults, its width, and the several hundred meters of topographic relief to the west and east, and in comparison to the other large fault-bounded basins in the system, with which its slip rates are similar (Fig. 5). Comparison of the magnitude of the observed ~10 mGal anomaly of the La Paz basin with the San Juan de los Planes and San José del Cabo basins (~25 and ~40 mGal, respectively) reflects this disparity in depth. The La Paz basin could be shallower because the El Carrizal fault became active later than the San Juan de los Planes and San José del Cabo faults or because it accommodates a lower slip rate; however, data summarized here and presented by Maloney (2009) show that the Carrizal and Los Planes faults have similar fault-slip rates. It is also possible that the Carrizal fault is more active farther north, and the gravity measures a less active southern part of the fault. Our favored interpretation is that the onshore Carrizal fault is a relatively young feature and thus has not accumulated sufficient slip to produce notable sedimentary accommodation space.

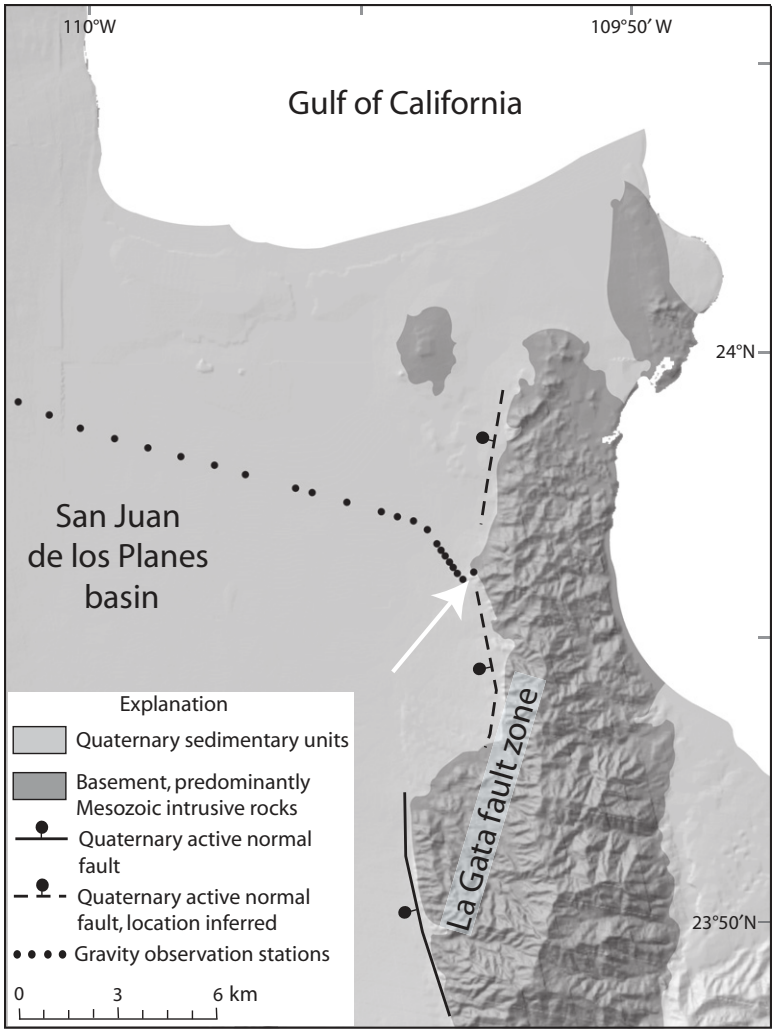

Figure 8. Gravity survey likely crosses La Gata fault (eastern basin-bounding fault) at a segment boundary, possibly causing eastern side of the basin to appear shallower than it actually is in other parts of the basin margin. White arrow points to inferred geometric segment boundary. Geology is from INEGI (1987).

Along all gravity models of the La Paz basin, the eastern basin is roughly twice the depth of the western basin; this is a contradiction to the basin topography because the El Carrizal fault, which controls the western basin, forms a well-developed escarpment (Maloney et al., 2007), whereas the Centenario fault, which controls the eastern basin, is subtly expressed in the landscape (Maloney, 2009). Three explanations can explain this apparent incongruity in relative basin depths. One possibility is that the Centenario fault formed prior to the Carrizal fault, accounting for the deeper basin adjacent to the Centenario fault than the Carrizal fault. A second explanation is that the Centenario fault accommodates higher slip rates than the Carrizal fault but is also subjected to higher erosion rates due to its proximity to a floodplain, where lateral erosion or sedimentation could explain the lack of preserved fault scarps.

We propose a third explanation, reflecting a more complex basin history. Earliest activity along the Carrizal fault may have occurred offshore along the northern stretch of this fault, leading to the formation of the deeper offshore La Paz basin (Gonzalez-Yajimovich et al., 2007). Faulting then progressed to the south and stepped eastward to the onshore Centenario fault, forming the deeper Centenario basin. The offshore portion of the Carrizal fault continued to lengthen toward the south, however, and eventually became active onshore. Once onshore activity along the Centenario and Carrizal faults began to overlap, the majority of activity became localized along the onshore Carrizal fault, while the Centenario fault became inactive (Fig. 10).

San José del Cabo Basin

The San José del Cabo basin is deeper than both the La Paz and the San Juan de los Planes basins and it exhibits the highest footwall topography adjacent to the basin, indicating that the San José del Cabo fault is likely more active than the Carrizal and San Juan de los Planes faults. Gravity data provide an estimate of 1.6–2.7 km for the maximum depth to bedrock of this basin (Fig. 6); however, when the present footwall relief as well as erosion of the footwall are taken into account, our gravity data provide results consistent with the lower end of the 5.2–6.5 km of Neogene differential uplift of the Cabo block, as estimated by Fletcher et al. (2000), but it is manifested across a wide system of faults, not only along the San José del Cabo fault.

The gravity data suggest that relict faults within the innermost San José del Cabo basin form a buried half graben (Fig. 6). As the San José del Cabo half graben evolved, it is likely that faulting began on the smaller relict faults within the basin, and the buried east-dipping fault under Santiago was the main basin-bounding fault (Fig. 6). Then, over time, faulting stepped westward and deformation became localized along the east-dipping San José del Cabo fault that bounds the west side of the basin, creating the half-graben structure that is reflected in the landscape. Alternatively, the fault buried under Santiago and the San José del Cabo fault may both be older faults that acted as a pair until the fault under Santiago died and the San José del Cabo fault became the sole active fault today.

COMPARISON TO OTHER YOUNG, ACTIVELY EXTENDING REGIONS

Gravity data suggest that both the San José del Cabo and San Juan de los Planes basins have significant intrabasin faults. These faults provide evidence that basins in the La Paz–Los Cabos region might have evolved in a similar manner as those in other regions. For example, half-graben rift basins in the Usangu Flats, Tanzania, part of the East African rift system, initiated as a synformal depression in which strain was distributed across a number of smaller faults (Morley, 2002). Over time, faults synthetic to the boundary fault accommodated most of the strain, while those antithetic to the boundary fault became inactive. Eventually, all deformation became localized along the boundary fault. In this style of rift basin evolution, the boundary fault developed relatively late during the evolution of the basin (Morley, 2002). A similar pattern is observed along the northern extension of the Red Sea Rift, which, like the Gulf of

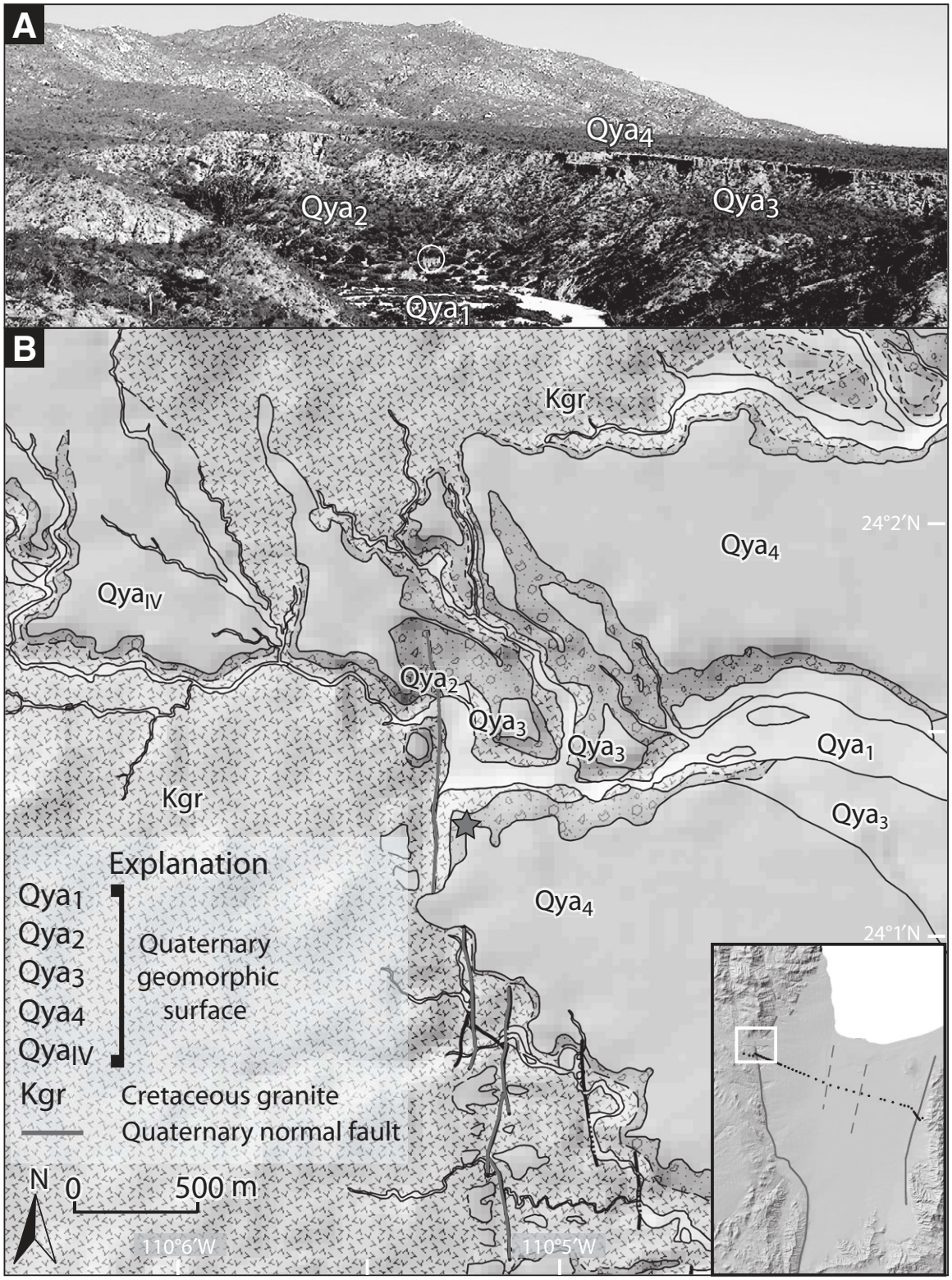

Figure 9. (A) Drainage incisions in the hanging wall of the fault reveal thin Quaternary cover over the granite bedrock. Star on geologic map marks location from which photograph was taken. Photograph was taken toward the north. For scale, white circle just below center of photograph highlights a two-story house (~8–10 m high). (B) Quaternary geologic map shows a section of the San Juan de los Planes fault zone. White box on inset location map shows geologic map location. Geologic map is from Busch et al. (2007). Inset location map geology is from INEGI (1987), and fault traces are from Busch et al. (2007).

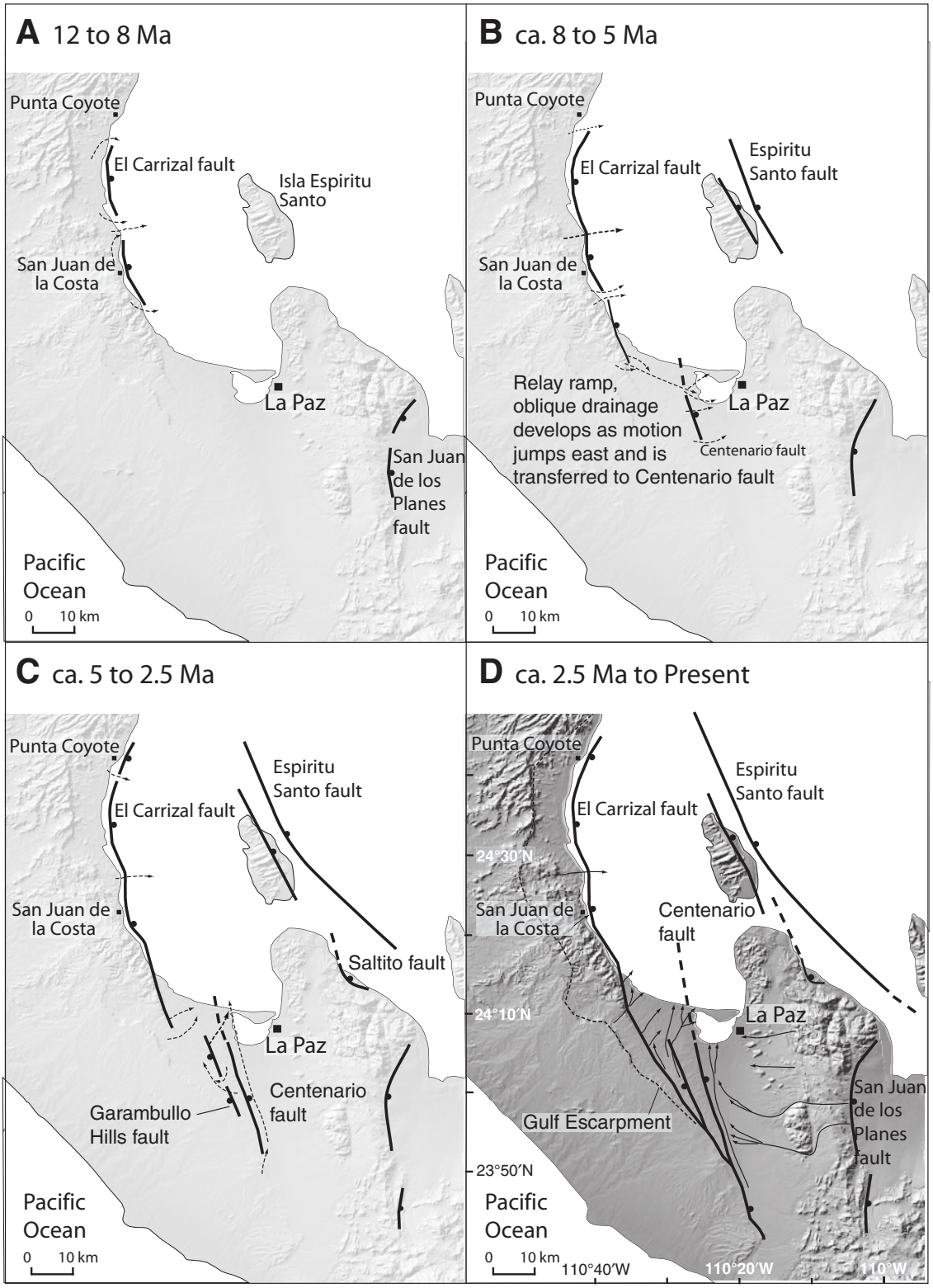

Figure 10. Tectonic evolution of the La Paz basin. Dashed lines in A–C represent drainage patterns, with arrows indicating transport direction. Modern drainages are solid in D. Base map is from Geomapapp (www.geomapapp.org). (A) The El Carrizal fault initiates offshore near the present-day location of San Juan de la Costa. Motion along this fault propagates north and south. (B) Motion on the El Carrizal fault jumps eastward, transferring strain to the Centenario fault. Onshore slip along the El Carrizal fault slows considerably as extension is accommodated primarily by the Centenario fault. Offshore slip along the El Carrizal fault continues. (C) Segments of the west-dipping Garambullo Hills fault begin to develop. (D) Onshore segments of the El Carrizal fault link up. Slip along the Garambullo Hills and Centenario faults slows or ceases as strain is transferred back to the El Carrizal fault. Presently, the La Paz basin is a half graben controlled by the El Carrizal fault on the west (after Maloney, 2009).

California, is a young, proto-oceanic rift trough (Leeder, 1995). Early in the development of the Hammam Faraun fault block, located along the east margin of the Gulf of Suez rift, intrablock fault zones had higher displacements than the border faults bounding the block; however, over time, deformation became localized along the boundary faults, and the intrabasin faults became inactive (Gawthorpe et al., 2003). In these young, actively extending regions, smaller intrabasin faults accommodate strain during the early stages of basin formation, and only later do the basin-bounding faults develop while the intrabasin faults die.

The basins within the La Paz–Los Cabos transect are fairly shallow (maximum displacements ranging from ~500 to 3000 m), but these values are not atypical compared to other young extensional basins. Extension in the Southern Apennines is accommodated by 20–45-km-long faults with maximum throws of 700–2100 m (Papanikolaou and Roberts, 2007) (Fig. 11). In addition, the faults bounding the rift blocks along the eastern side of the Gulf of Suez rift are of similar length and spacing to those along the southwest margin of the Gulf of California and have a maximum throw ranging from ~500 m to 4800 m (Moustafa, 1993). Two belts of faults bound the east-margin rift blocks of the Gulf of Suez rift. One belt is considered to be the rift-bounding faults, whereas the other belt bounds the coastal blocks and is situated closer to the rift axis. The faults that bound the coastal blocks have a greater throw than the rift-bounding faults, indicating that the deformation rate increases toward the rift axis (Moustafa, 1993; Gawthorpe et al., 2003). The western margin of the southern Gulf of Suez shows a similar structural pattern (Bosworth et al., 2005).

The marginal fault system adjacent to the Gulf of California exhibits structural similarities to the margin of the Gulf of Suez rift. That is, the San Juan de los Planes and La Paz faults might be analogous to the lower displacement rift-bounding faults of the east margin of the Gulf of Suez rift, and the San José del Cabo and Espiritú Santo faults accommodate a higher deformation rate and greater displacement, like the faults that bound the coastal blocks of the Gulf of Suez rift.

FAULT SYSTEM EVOLUTION

Even though these gravity data and interpreted basin models provide only a reconnaissance-level view of the onshore structure of three major normal-fault–bounded basins in the La Paz–Los Cabos transect, we are able to draw critical conclusions about the structural evolution of the system. The San Juan de los Planes and San José del Cabo basins likely began forming along smaller faults that are now buried within the basin center. As rifting progressed, faulting moved outward from the basin center, and eventually strain became localized along the present-day boundary faults. This process either involved a true stepping from central faults outward, or paired faults in which the central faults die and the boundary faults continue being active. The onshore portion of the La Paz basin is inferred to have formed as faulting stepped westward, with activity initiating along the Centenario fault, but later transferring to the more westerly El Carrizal fault. Because the San José del Cabo basin is the deepest with the highest adjacent footwall topography, it is likely the most active of the major normal faults within this gulf-margin system, and/or it may also have become active earlier than the other basin-bounding faults.

The late Quaternary slip rates along the San Juan de los Planes fault (Busch et al., 2008) and the Carrizal fault (Maloney et al., 2007) are comparable (~0.1–1.0 mm/yr). If we assume that these rates represent the long-term average slip rates along the basin-bounding fault systems, when combined with the maximum depth to bedrock for each basin, they indicate that these two basins began forming ca. 2–5 Ma (assuming a constant slip rate), though it is possible that the northern section of the Carrizal fault began forming earlier than the southern, as discussed already.

Martínez Gutiérrez and Sethi (1997) examined the sedimentary rocks within the San José del Cabo basin to infer the basin history and documented middle-late Miocene sediments as the oldest sedimentary deposit within the basin, indicating that basin subsidence began in the middle-late Miocene. They also observed high-gradient, alluvial-fan deposits of the upper Pliocene–lower Pleistocene Los Barriles Formation and inferred that these sediments represent the onset of the formation of the San José del Cabo fault. Martínez Gutiérrez and Sethi's (1997) observations support our interpretation of basin formation initiating along faults within the basin and later localizing along the present-day basin-bounding fault.

The timing of formation of the La Paz and San Juan de los Planes basins (2–5 Ma) based on extrapolation from slip rates and depth to bedrock is incongruent with the timing of initiation of the San José del Cabo basin (middle-late Miocene). It is possible, then, that the slip rates along the San Juan de los Planes and Carrizal faults (from which our estimate is derived) are not constant over time and along strike, therefore rendering our extrapolation an invalid estimate of the timing of basin formation. An alternative explanation is that the San José del Cabo basin began forming earlier than the San Juan de los Planes and La Paz basins. The lack of observed Miocene sediments within these basins (though they could be buried) provides support for more recent formation of the San Juan de los Planes and La Paz basins. At 3.6–2.4 Ma, oceanic crust began forming along the Alarcón Rise (DeMets, 1995; Umhoefer et al., 2008), and yet faulting has remained active in the gulf-margin system.

Like the Gulf of California, the Reykjanes Ridge in Iceland is an obliquely spreading mid-ocean ridge that is marked by a fracture population marginal to the main rift zone that differs in orientation from the fractures within the main zone of deformation (Tuckwell et al., 1998; Clifton and Schlische, 2003). Numerical and clay modeling of the fracture populations along the Reykjanes Ridge supports the idea that their behavior is consistent with the observation that crust along the rift margin is thicker, cooler, and denser than that within the rift axis. These differing crustal properties between the main deformation zone and the marginal zone cause stress differences in these two regions, resulting in distributed deformation within the transition zone that is oriented differently from that within the axis of deformation (Tuckwell et al., 1998; Clifton and Schlische, 2003). Like the Reykjanes Ridge, as the gulf-axis fault system in the southern gulf became more well developed, a greater topographic and temperature gradient may have been created between the thinned crust in the main rift zone and the thicker continental crust marginal to the main zone of rifting. This contrast in crustal type, thickness, and temperature may drive the continued activity along this low-slip, marginal normal-fault array.

CONCLUSIONS

An array of roughly north-striking, left-stepping normal faults along the southwest margin of the Gulf of California accommodates onshore, rift-related extension at relatively low rates compared to the gulf-axis system. Gravity surveys across the basins bounded by these normal faults reveal basin depths ranging from ~500 to 3000 m. The San José del Cabo basin is the deepest, and the La Paz basin is the shallowest. Slip rates, as estimated with OSL dating techniques and fault scarp heights, are comparable between the La Paz and San Juan de los Planes faults and, when coupled with the basin depths, suggest that these basins may have begun forming ca. 2–5 Ma (assuming a constant slip rate). Buried faults are present within these basins, indicating that during the early stages of basin formation, strain was probably distributed across a number of smaller intrabasin faults. Late in the evolution of the basin, the basin-bounding

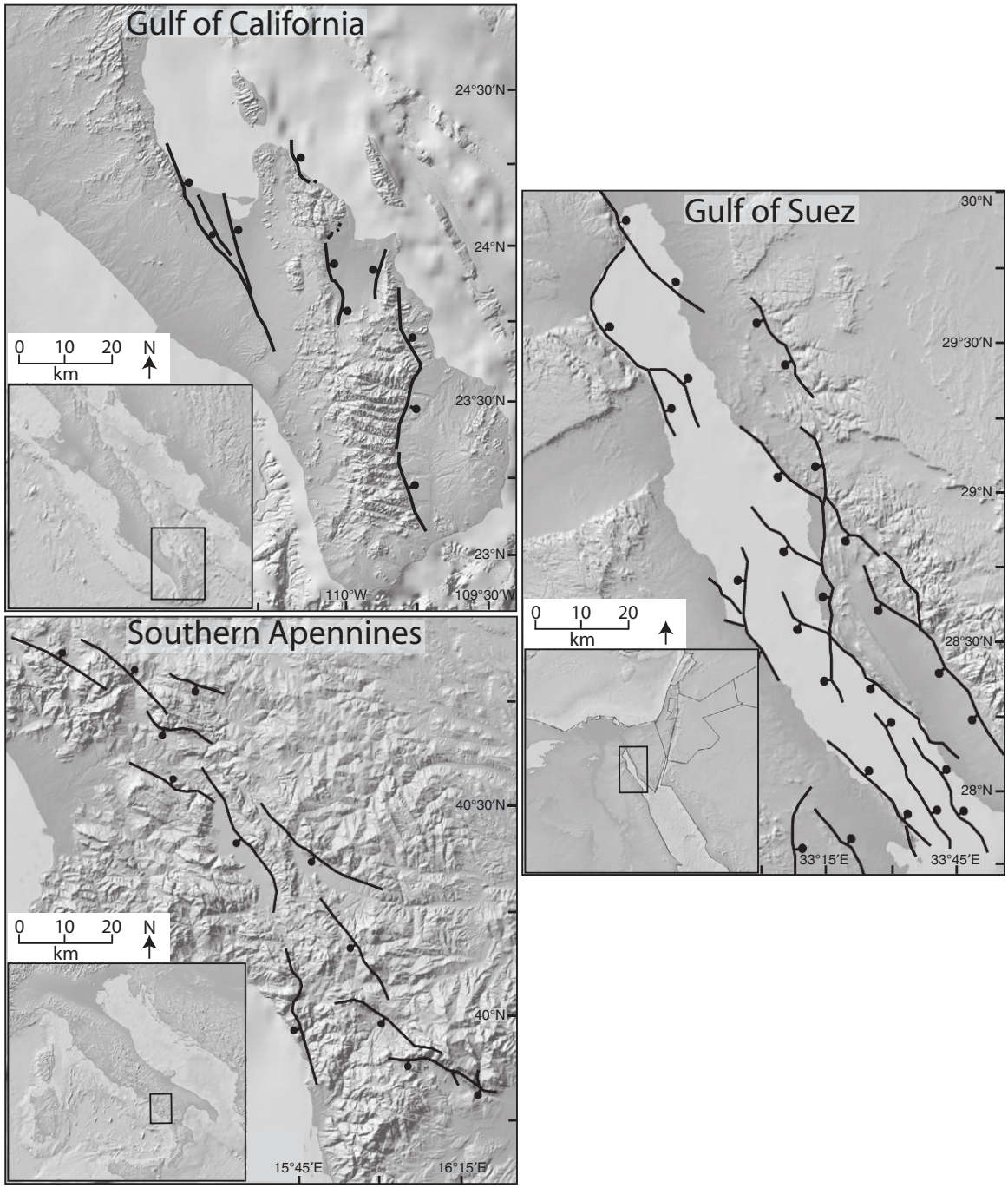

Figure 11. Comparison of distributed active fault trace geometry in extensional regions. Fault length and spacing are comparable among these areas, and faults accommodate comparable displacements, ranging from ~500 to 5000 m. Base maps are from GeoMapApp (www.geomapapp.org). Baja Peninsula fault traces are from INEGI (1987); Busch et al. (2006, 2007); and Maloney et al. (2007). Gulf of Suez fault traces were modified from Bosworth et al. (2005). Southern Apennines fault traces are from Papanikolaou and Roberts (2007).

faults developed, and the intrabasin faults died. Whereas the gulf-margin system contributes modestly to the total active extension across the Gulf Extensional Province, it shows sustained, low-rate, active faulting and landscape and sedimentary basin evolution (including the highest topographic relief in the southern Baja California peninsula) across a fault array situated in a zone of transition in crustal thickness and material properties.

ACKNOWLEDGMENTS

We are grateful to Mike Taylor and an anonymous reviewer for comments that helped to improve this paper. Thanks are due to Jim Tyburczy for advice and review on gravity processing and for the loan of the Lacoste and Romberg Model G gravity meter. Sarah Robinson digitized the geologic map in Figure 6. Discussions with Ernesto Ramos were helpful. This research was supported by U.S. National Science Foundation Margins grants to Umhoefer and Arrowsmith. Base maps in Figures 1 and 11 were produced using GeoMapApp.

REFERENCES CITED

Anderson, E.M., 1951, The Dynamics of Faulting and Dyke Formation, with Applications to Britain: Edinburgh, Oliver & Boyd, 206 p.

Angelier, J., Colletta, B., Chorowicz, J., Ortlieb, L., and Rangin, C., 1981, Fault tectonics of the Baja California peninsula and the opening of the Sea of Cortez, Mexico: Journal of Structural Geology, v. 3, no. 4, p. 347–357, doi:10.1016/0191-8141(81)90035-3.

Arrowsmith, J.R., Busch, M.M., Umhoefer, P.J., Kent, G., Driscoll, N., Martínez-Gutiérrez, G., Maloney, S.J., and Buchanan, B., 2009, Active faulting and seismicity across the SW Gulf of California plate margin: Anomalous rifting at slow geologic rates 2–3 m.y. after spreading initiated [abs.]: Eos (Transactions, American Geophysical Union), v. 90, no. 52, fall meeting supplement, abstract T33E-08.

Atwater, T., 1970, Implications of plate tectonics for the Cenozoic tectonic evolution of western North America: Geological Society of America Bulletin, v. 81, p. 3513–3536, doi:10.1130/0016-7606(1970)81[3513:IOPTFT]2.0.CO;2.

Bosworth, W., Huchon, P., and McClay, K., 2005, The Red Sea and Gulf of Aden basins: Journal of African Earth Sciences, v. 43, p. 334–378, doi:10.1016/j.jafrearsci.2005.07.020.

Bronk Ramsey, C., 1995, Radiocarbon calibration and analysis of stratigraphy: The OxCal program: Radiocarbon, v. 37, no. 2, p. 425–430.

Bronk Ramsey, C., 2001, Development of the radiocarbon calibration program OxCal: Radiocarbon, v. 43, no. 2A, p. 355–363.

Bronk Ramsey, C., 2008, Deposition models for chronological records: Quaternary Science Reviews, v. 27, no. 1–2, p. 42–60, doi:10.1016/j.quascirev.2007.01.019.

Buchanan, B., 2010, Uplifted Marine Terraces and Active Faulting along Southwestern La Paz Bay, Baja California Sur, Mexico [M.S. thesis]: Flagstaff, Arizona, Northern Arizona University, 190 p.

Burbank, D.W., and Anderson, R.S., 2001, Tectonic Geomorphology: Oxford, Blackwell Scientific, 270 p.

Burger, H.R., Sheehan, A.F., and Jones, C.H., 2006, Introduction to Applied Geophysics: Exploring the Shallow Subsurface: New York, W.W. Norton & Company, 600 p.

Busch, M.M., Arrowsmith, J.R., Umhoefer, P.J., Martínez-Gutiérrez, G., Toké, N.A., Brothers, D., DiMaggio, E.N., Maloney, S.J., Zielke, O., and Buchanan, B., 2006, Late Quaternary faulting in the Cabo San Lucas–La Paz region, Baja California [abs.]: Eos (Transactions, American Geophysical Union), v. 87, no. 52, fall meeting supplement, abstract T41D-1612.

Busch, M.M., Coyan, J.A., Arrowsmith, J.R., Maloney, S.J., Martínez-Gutiérrez, G., and Umhoefer, P.J., 2007, Late Quaternary faulting along the San Juan de los Planes fault zone, Baja California Sur, Mexico [abs.]: Eos (Transactions, American Geophysical Union, v. 88, no. 52, fall meeting supplement, abstract T41A-0357.

Busch, M.M., Coyan, J.A., Arrowsmith, J.R., Umhoefer, P.J., and Martínez-Gutiérrez, G., 2008, Normal fault basin geometries from gravity analyses in the La Paz–Los Cabos region, Baja California Sur, Mexico [abs.]: Eos (Transactions, American Geophysical Union), v. 89, no. 53, fall meeting supplement, abstract T13E-02.

Clifton, A.E., and Schlische, R.W., 2001, Nucleation, growth, and linkage of faults in oblique rift zones: Results from experimental clay models and implications for maximum fault size: Geology, v. 29, no. 5, p. 455–458, doi:10.1130/0091-7613(2001)029<0455:NGALOF>2.0.CO;2.

Clifton, A.E., and Schlische, R.W., 2003, Fracture populations on the Reykjanes Peninsula, Iceland: Comparison with experimental clay models of oblique rifting: Journal of Geophysical Research, v. 108, no. B2, doi:10.1029/2001JB000635.

Clifton, A.E., Schlische, R.W., Withjack, M.O., and Ackermann, R.V., 2000, Influence of rift obliquity on fault-population systematics: Results of experimental clay models: Journal of Structural Geology, v. 22, p. 1491–1509, doi:10.1016/S0191-8141(00)00043-2.

Cogbill, A.H., 1990, Gravity terrain corrections calculated using digital elevation models: Geophysics, v. 55, no. 1, p. 102–106, doi:10.1190/1.1442762.

DeDiego-Forbis, T., Douglas, R., Gorsline, D., Nava-Sanchez, E., Mack, L., and Banner, J., 2004, Late Pleistocene (Last Interglacial) terrace deposits, Bahía Coyote, Baja California Sur, México: Quaternary International, v. 120, p. 29–40, doi:10.1016/j.quaint.2004.01.004.

DeMets, C., 1995, A reappraisal of seafloor spreading lineations in the Gulf of California: Implications for the transfer of Baja California to the Pacific plate and estimates of Pacific–North America motion: Geophysical Research Letters, v. 22, no. 24, p. 3545–3548, doi:10.1029/95GL03323.

Densmore, A.L., Dawers, N.H., Gupta, S., Guidon, R., and Goldin, T., 2004, Footwall topographic development during continental extension: Journal of Geophysical Research, v. 109, p. F03001, doi:10.1029/2003JF000115.

Drake, W., 2005, Structural Analysis, Stratigraphy, and Geochemistry of the San José Island Accommodation Zone, Baja California Sur, Mexico [M.S. thesis]: Flagstaff, Northern Arizona University, 231 p.

Fletcher, J.M., and Munguía, L., 2000, Active continental rifting in southern Baja California, Mexico: Implications for plate motion partitioning and the transition to seafloor spreading in the Gulf of California: Tectonics, v. 19, no. 6, p. 1107–1123, doi:10.1029/1999TC001131.

Fletcher, J.M., Kohn, B.P., Foster, D.A., and Gleadow, A.J.W., 2000, Heterogeneous Neogene cooling and exhumation of the Los Cabos block, southern Baja California: Evidence from fission-track thermochronology: Geology, v. 28, no. 2, p. 107–110, doi:10.1130/0091-7613(2000)28<107:HNCAEO>2.0.CO;2.

Fletcher, J.M., Pérez-Venzor, J.A., Gonzáles-Barba, G., and Aranda-Gómez, J.J., 2003, Ridge-trench interactions and the ongoing capture of the Baja California microplate—New insights from the southern Gulf extensional province, *in* Geologic Transects across Cordilleran México, Guidebook for Field Trips of the 99th Geological Society of America Cordilleran Section Annual Meeting, Puerto Vallarta, Jalisco, México, 29–31 March 2003: Mexico, D.F., Universidad Nacional Autónoma de México, Instituto de Geologia, Publicación Especial 1, Field Trip 2, p. 13–31.

Fletcher, J.M., Grove, M., Kimbrough, D., Lovera, O., and Gehrels, G.E., 2007, Ridge-trench interactions and the Neogene tectonic evolution of the Magdalena shelf and southern Gulf of California: Insights from detrital zircon U-Pb ages from the Magdalena fan and adjacent areas: Geological Society of America Bulletin, v. 119, p. 1313–1336, doi:10.1130/B26067.1.

Forman, S.L., Pierson, J., and Lepper, K., 2000, Luminescence geochronology, *in* Sowers, J.M., Noller, J.S., and Lettis, W.R., eds., Quaternary Geochronology: Methods and Applications: Washington, D.C., American Geophysical Union Reference Shelf 4, p. 157–176.

Gallardo, L.A., Pérez-Flores, M.A., and Gómez-Treviño, E., 2005, Refinement of three-dimensional multilayer models of basins and crustal environments by inversion of gravity and magnetic data: Tectonophysics, v. 397, p. 37–54, doi:10.1016/j.tecto.2004.10.010.

Gawthorpe, R.L., and Leeder, M.R., 2000, Tectono-sedimentary evolution of active extensional basins: Basin Research, v. 12, p. 195–218, doi:10.1046/j.1365-2117.2000.00121.x.

Gawthorpe, R.L., Jackson, C.H.-L., Young, M.J., Sharp, I.R., Moustafa, A.R., and Leppard, C.W., 2003, Normal fault growth, displacement localization and the evolution of normal fault populations: The Hammam Faraun fault block, Suez rift, Egypt: Journal of Structural Geology, v. 25, p. 883–895, doi:10.1016/S0191-8141(02)00088-3.

Goble, R.J., and Rittenour, T.M., 2006, A linear modulation OSL study of the unstable ultrafast component in samples from glacial Lake Hitchcock, Massachusetts, USA: Ancient TL, v. 24, no. 2, p. 37–46.

Gonzalez-Yajimovich, O.E., Gorsline, D.S., and Douglas, R.G., 2007, Frequency and sources of basin floor turbidites in Alfonso Basin, Gulf of California, Mexico: Products of slope failures: Sedimentary Geology, v. 199, p. 91–105, doi:10.1016/j.sedgeo.2005.09.025.

Gupta, S., Cowie, P.A., Dawers, N.H., and Underhill, J.R., 1998, A mechanism to explain rift-basin subsidence and stratigraphic patterns through fault-array evolution: Geology, v. 26, no. 7, p. 595–598, doi:10.1130/0091-7613(1998)026<0595:AMTERB>2.3.CO;2.

Hausback, B.P., 1984, Cenozoic Volcanic and Tectonic Evolution of Baja California Sur, Mexico [Ph.D. thesis]: Berkeley, University of California, 72 p.

Ingersoll, R.V., and Busby, C.J., 1995, Tectonics of sedimentary basins, *in* Busby, C.J., and Ingersoll, R.V., eds., Tectonics of Sedimentary Basins: Cambridge, UK, Blackwell Science, 579 p.

Instituto Nacional de Estadistica, Geografia e Informatica (INEGI), 1987, Carta Geologica, San Jose del Cabo: Aguascalientes, Mexico, Instituto Nacional de Estadistica, Geografia e Informatica, scale 1:250,000.

Jackson, J.A., and McKenzie, D.P., 1983, The geometrical evolution of normal fault systems: Journal of Structural Geology, v. 5, p. 471–482, doi:10.1016/0191-8141(83)90053-6.

Jackson, J.A., and White, N.J., 1989, Normal faulting in the upper continental crust: Observations from regions of active extension: Journal of Structural Geology, v. 11, p. 15–36, doi:10.1016/0191-8141(89)90033-3.

LaCoste and Romberg, LLC, 2004, Instructional Manual: Model G & D Gravity Meters: Austin, Texas, LaCoste and Romberg, 127 p.

Leeder, M.R., 1995, Continental rifts and proto-oceanic rift troughs, *in* Busby, C.J., and Ingersoll, R.V., eds., Tectonics Of Sedimentary Basins: Cambridge, UK, Blackwell Science, 579 p.

Lian, O.B., and Roberts, R.G., 2006, Dating the Quaternary: Progress in luminescence dating of sediments: Quaternary Science Reviews, v. 25, p. 2449–2468, doi:10.1016/j.quascirev.2005.11.013.

Lizarralde, D., Axen, G.J., Brown, H.E., Fletcher, J.M., González-Fernández, A., Harding, A.J., Holbrook, W.S., Kent, G.M., Paramo, P., Sutherland, F., and Umhoefer, P.J., 2007, Variation in styles of rifting in the Gulf of California: Nature, v. 448, p. 466–469, doi:10.1038/nature06035.

Maloney, S.J., 2009, Late Quaternary Faulting History of the Northern El Carrizal Fault, Baja California Sur, Mexico [M.S. thesis]: Flagstaff, Northern Arizona University, 196 p.

Maloney, S.J., Umhoefer, P.J., Arrowsmith, J.R., Martinez-Gutiérrez, G., Santillanez, A.U., and Rittenour, T.R., 2007, Late Pleistocene–Holocene faulting history along the northern El Carrizal fault, Baja California Sur, Mexico: Earthquake recurrence at a persistently active

rifted margin [abs.]: Eos (Transactions, American Geophysical Union), v. 88, no. 52, fall meeting supplement, abstract T41A-0357.

Martínez-Gutiérrez, G., and Sethi, P.S., 1997, Miocene-Pleistocene sediments within the San José del Cabo Basin, Baja California Sur, Mexico, *in* Johnson, M.E., and Ledesma-Vázquez, J., eds., Pliocene Carbonates and Related Facies Flanking the Gulf of California, Baja California, Mexico: Boulder, Colorado, Geological Society of America Special Paper 318, p. 141–166.

Mayer, L., and Vincent, K.R., 1999, Active tectonics of the Loreto area, Baja California Sur, Mexico: Geomorphology, v. 27, p. 243–255, doi:10.1016/S0169-555X(98)00074-9.

McClay, K.R., Dooley, T., Whitehouse, P., and Mills, M., 2002, 4-D evolution of rift systems: Insights from scaled physical models: American Association of Petroleum Geologists Bulletin, v. 86, no. 6, p. 935–959.

McTeague, M., 2006, Marginal Strata of the East Central San Jose del Cabo Basin, Baja California Sur, Mexico [M.S. thesis]: Flagstaff, Northern Arizona University, 152 p.

Morley, C.K., 2002, Evolution of large normal faults: Evidence from seismic reflection data: American Association of Petroleum Geologists Bulletin, v. 86, no. 6, p. 961–978.

Moustafa, A.R., 1993, Structural characteristics and tectonic evolution of the east-margin blocks of the Suez rift: Tectonophysics, v. 223, p. 381–399, doi:10.1016/0040-1951(93)90146-B.

Munguía, L.M., González, M., Mayer, S., and Aguirre, A., 2006, Seismicity and state of stress in the La Paz–Los Cabos region, Baja California Sur, Mexico: Bulletin of the Seismological Society of America, v. 96, no. 2, p. 624–636, doi:10.1785/0120050114.

Oskin, M., Stock, J.M., and Martín-Barajas, A., 2001, Rapid localization of Pacific–North America plate motion in the Gulf of California: Geology, v. 29, p. 459–462, doi:10.1130/0091-7613(2001)029<0459:RLOPNA>2.0.CO;2.

Papanikolaou, I.D., and Roberts, G.P., 2007, Geometry, kinematics and deformation rates along the active normal fault system in the Southern Apennines: Implications for fault growth: Journal of Structural Geology, v. 29, p. 166–188, doi:10.1016/j.jsg.2006.07.009.

Plattner, C., Malservisi, R., Dixon, T.H., LaFemina, P., Sella, G.F., Fletcher, J., and Suarez-Vidal, F., 2007, New constraints on relative motion between the Pacific plate and Baja California microplate (Mexico) from GPS measurements: Geophysical Journal International, v. 170, no. 3, p. 1373–1380, doi:10.1111/j.1365-246X.2007.03494.x.

Reimer, P., Baillie, M., Bard, E., Bayliss, A., Beck, J., Bertrand, C., Blackwell, P., Buck, C., Burr, G., Cutler, K., Damon, P., Edwards, R., Fairbanks, R., Friedrich, M., Guilderson, T., Hogg, A., Hughen, K., Kromer, B., McCormac, G., Manning, S., Bronk Ramsey, C., Reimer, R., Remmele, S., Southon, J., Stuiver, M., and Talamo, S., 2004, Intcal04 terrestrial radiocarbon age calibration, 0–26 cal kyr BP: Radiocarbon, v. 46, no. 3, p. 1029–1058.

Sharma, P.V., 1997, Environmental and Engineering Geophysics: Cambridge, UK, Cambridge University Press, 500 p.

Stock, J.M., and Hodges, K.V., 1989, Pre-Pliocene extension around the Gulf of California and the transfer of Baja California to the Pacific plate: Tectonics, v. 8, no. 1, p. 99–115, doi:10.1029/TC008i001p00099.

Stock, J.M., and Lee, J., 1994, Do microplates in subduction zones leave a geological record?: Tectonics, v. 13, p. 1472–1488, doi:10.1029/94TC01808.

Tatlow, M.A., 2000, Measuring Depth to Bedrock Using Gravity Methods in a Remediation Study Area in Phoenix, Arizona [M.S. thesis]: Tempe, Arizona State University, 132 p.

Tuckwell, G.W., Bull, J.M., and Sanderson, D.J., 1998, Numerical models of faulting at oblique spreading centers: Journal of Geophysical Research, v. 103, no. B7, p. 15,473–15,482, doi:10.1029/97JB03673.

Umhoefer, P.J., Mayer, L., and Dorsey, R.J., 2002, Evolution of the margin of the Gulf of California near Loreto, Baja California peninsula, Mexico: Geological Society of America Bulletin, v. 114, p. 849–868, doi:10.1130/0016-7606(2002)114<0849:EOTMOT>2.0.CO;2.

Umhoefer, P.J., Sutherland, F., Kent, G., Harding, A., Lizarralde, D., Schwennicke, T., Fletcher, J., Holbrook, W.S., and Axen, G., 2008, Synchronous changes in rift-margin basins and initiation of the Alarcón spreading ridge and related transform fault, southwestern Gulf of California: Geological Society of America Abstracts with Programs, v. 40, no. 6, p. 151.

Withjack, M.O., and Jamison, W.R., 1986, Deformation produced by oblique rifting: Tectonophysics, v. 126, p. 99–124, doi:10.1016/0040-1951(86)90222-2.

MANUSCRIPT RECEIVED 27 MAY 2010
REVISED MANUSCRIPT RECEIVED 15 OCTOBER 2010
MANUSCRIPT ACCEPTED 19 OCTOBER 2010

Printed in the USA